

When Single Answer Is Not Enough: Rethinking Single-Step Retrosynthesis Benchmarks for LLMs

Bogdan Zagribelnyy¹ Ivan Ilin¹ Maksim Kuznetsov² Nikita Bondarev¹ Roman Schutski³
 Thomas MacDougall² Rim Shayakhmetov¹ Zulfat Miftahutdinov² Mikolaj Mizera³ Vladimir Aladinskiy¹
 Alex Aliper¹ Alex Zhavoronkov^{1,2,3}

Abstract

Recent progress has expanded the use of large language models (LLMs) in drug discovery, including synthesis planning. However, objective evaluation of retrosynthesis performance remains limited. Existing benchmarks and metrics typically rely on published synthetic procedures and Top-K accuracy based on single ground-truth, which does not capture the open-ended nature of real-world synthesis planning. We propose a new benchmarking framework for single-step retrosynthesis that evaluates both general-purpose and chemistry-specialized LLMs using ChemCensor, a novel metric for chemical plausibility. By emphasizing plausibility over exact match, this approach better aligns with human synthesis planning practices. We also introduce CREED, a novel dataset comprising millions of ChemCensor-validated reaction records for LLM training, and use it to train a model that improves over the LLM baselines under this benchmark.

1. Introduction

The modern small molecule drug development process requires thoughtful control over the synthetic accessibility of the designed molecules (Gao & Coley, 2020). In practice, synthetic feasibility is assessed through synthesis planning, most prominently retrosynthetic analysis (Vléduts, 1963; Corey, 1967). Computer-aided synthesis planning (CASP) aims to automate this process by proposing routes to available building blocks (Tu et al., 2023). While direct multistep

¹Insilico Medicine AI Limited, Level 6, Unit 08, Block A, IRENA HQ Building, Masdar City, Abu Dhabi, UAE ²Insilico Medicine Canada Inc., 3710-1250 René-Lévesque Blvd W, Montreal, Quebec, H3B 4W8, Canada ³Insilico Medicine Hong Kong Ltd., Unit 310, 3/F, Building 8W, Phase 2, Hong Kong Science Park, Pak Shek Kok, New Territories, Hong Kong, Hong Kong SAR, China. Correspondence to: Maksim Kuznetsov <kuznetsov@insilicomedicine.com>.

Preprint. February 4, 2026.

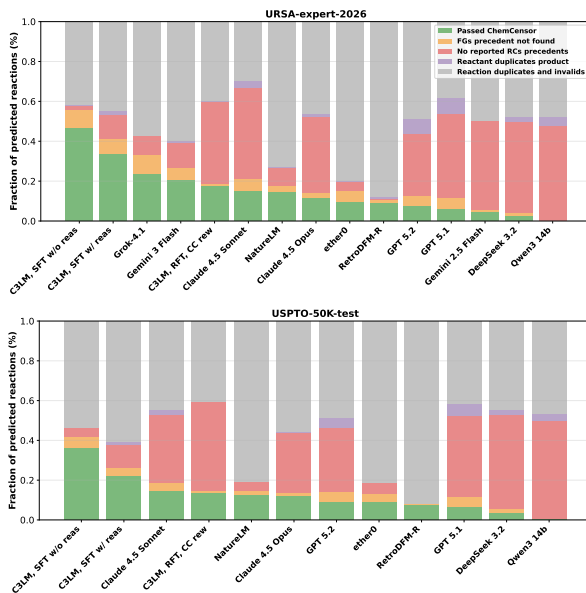


Figure 1. Assessment of generated reactants from benchmarked models by ChemCensor; each answer is assigned to pass or specific non-pass categories, and models are ordered by the fraction of ChemCensor passed reactions.

models are emerging (Shee et al., 2025), many CASP tools still decompose the problem into (i) *single-step retrosynthesis* (SSRS), which proposes candidate disconnections, and (ii) *multistep retrosynthesis* (MSRS), which assembles these steps into complete routes (Zhong et al., 2024).

Despite substantial progress and industrial adoption of CASP systems (Grzybowski et al., 2018), their evaluation remains a bottleneck (Maziarz et al., 2025). Reliable automated assessment is difficult because reaction databases are incomplete and heterogeneous, reactivity depends strongly on molecular context, and expert review is costly and hard to scale (Maziarz et al., 2025). As a result, benchmarking practices are fragmented and often hard to reproduce across models, datasets, and planners (Jiang et al., 2023).

Commonly used metrics, including Top-K exact-match accuracy for SSRS (Segler & Waller, 2017), solvability for

MSRS (Segler et al., 2018; Choe et al., 2025), and related variants (Schwaller et al., 2020), provide only indirect and limited signals of chemical plausibility (Morgunov & Batista, 2025). In particular, exact-match metrics implicitly assume a single “ground-truth” disconnection, even though many targets admit multiple valid retrosynthetic choices, and they do not directly test key chemical criteria such as reaction-center validity, functional-group compatibility, and chemo-/regio-/stereoselectivity (Westerlund et al., 2025; Maziarz et al., 2025). Expert databases and rule-based tools (e.g., Reaxys (Elsevier), SciFinder (Chemical Abstracts Service (CAS))) can support detailed reaction-by-reaction analysis, but they are not designed for continuous, automated benchmarking of model outputs at scale.

The rise of large language models (LLMs) (Wolf et al., 2020; Brown et al., 2020a), their flourishing variety and continuous emergence of new LLMs alongside the claims of their potential applicability in the synthetic planning domain (Xuan-Vu et al., 2025) demands unprecedented benchmarking approaches to objectively assess the performance of LLMs in real-world out-of-domain (OOD) tasks of retrosynthetic analysis applied to the drug discovery process, since the disadvantages of the traditional USPTO-50K test are recognized by the community (Torren-Peraire et al., 2024).

In our study, we utilize the new metric called ChemCensor as an alternative to traditional Top-K accuracy to assess SSRS outputs of LLMs, emphasizing the detrimental impact of “ground truth” dogma promoted by Top-K accuracy. ChemCensor enables benchmarking with broader chemical context augmentation and structured benchmark compound sets creation exemplified by the **URSA-expert-2026** set of 100 completely novel molecular structures with expert assessment of their synthetic feasibility. The unique chemical reactions dataset **CREED** of unprecedented size ($\sim 6.4\text{M}$) and reliability was created using $\sim 3\text{K}$ in-house reaction templates and verified by ChemCensor. The CREED was used to fine-tune the novel **C3LM** language model, outperforming general-purpose foundation and the chemical generalist models.

The key contributions of our work are as follows:

1. We propose **ChemCensor**, a metric for evaluating single-step retrosynthesis predictions beyond exact-match Top-K accuracy.
2. We construct **CREED**, a 6M template-derived reaction dataset verified with ChemCensor.
3. We release **URSA-expert-2026**, an expert-annotated benchmark of 100 novel targets for SSRS evaluation.
4. We train the **C3LM** model on the **CREED**, improving the performance over general-purpose LLMs and chemical generalist models.

2. Related Work

2.1. Benchmarking solutions for SSRS

Metrics. Top-K accuracy (Segler & Waller, 2017) is a standard evaluation metric for SSRS. For each product molecule, a model outputs an ordered list of candidate precursor (reactant) sets ranked by confidence; Top-K accuracy reports the fraction of test cases in which the recorded ground-truth precursor set appears among the top K predictions.

Round-trip accuracy is an evaluation metric that measures whether a retrosynthesis model’s predicted reactants can be forward-validated by a reaction prediction model (Schwaller et al., 2020). It quantifies the percentage of retrosynthesis predictions that, when passed through a forward reaction model, reproduce the original product.

Beyond exact-match Top-K, several works advocate distribution- and diversity-aware evaluation to better reflect how a model behaves as a generator of chemically meaningful suggestions (Schwaller et al., 2019b). In this line, coverage quantifies how broadly the model explores reaction space, for example, as the fraction of reaction classes (or templates) present in the reference set that also appear among the model’s predictions (Hastedt et al., 2024). Class diversity captures how varied the predicted chemistry is, helping detect mode collapse where a model repeatedly proposes the same few transformations. Finally, the Jensen–Shannon divergence (Lin, 1991) measures how closely the distribution of predicted reaction classes matches the reference distribution.

The MaxFrag accuracy (Tetko et al., 2020) emphasizes the largest fragment in the predicted reactant set, offering a targeted evaluation that is less influenced by ambiguous or unclear reagent information in USPTO-based reaction sets. This metric is particularly useful when annotation noise or reagent ambiguity can obscure the true performance of retrosynthetic models. In a different approach (Liu et al., 2023), SSRS models are evaluated via linkage to a search algorithm in terms of exact reaction-match accuracy across the rebuilt reaction network from USPTO. Nevertheless, both the latter approach and MaxFrag accuracy inherit the “ground-truth” dogma of the Top-K accuracy metric.

Recent LLM-style retrosynthesis papers (Zhao et al., 2025b; Lin et al., 2025) report a broad suite of evaluation metrics, including exact match, BLEU (Papineni et al., 2002), Levenshtein edit distance (Levenshtein, 1966), and molecular similarity-based scores computed between the predicted precursor set and the corresponding ground-truth precursors.

Benchmarking infrastructure. Syntheseus is an open, modular benchmarking platform designed to evaluate and compare SSRS models and MSRS planning algorithms under standardized and reproducible conditions (Maziarz et al.,

2025). In addition to classic Top-K accuracy, Syntheseus reports ranking-based metrics such as Mean Reciprocal Rank (MRR), which captures how highly a model places the first correct answer in its ranked list of predictions.

2.2. LLMs for the SSRS task

The sequential representation of molecules via SMILES enables single-step retrosynthesis to be formulated as product-to-reactant translation with Transformer-style LLMs, typically trained through large-scale pretraining and then adapted by instruction tuning or reaction-specific fine-tuning on patent reaction corpora - e.g., USPTO-derived sets. Recent work spans (i) *generalist or science foundation* models, including NatureLM (Xia et al., 2025), nach0 (Livne et al., 2024), and ChemDFM (Zhao et al., 2025b), can be adapted to retrosynthesis; (ii) *data-augmentation* strategies that expand reaction supervision, including template-/rule-driven large-scale generation and pretraining in RSGPT (Deng et al., 2025) as well as fragment/recombination-style augmentation and joint reaction–retrosynthesis training objectives in ChemDual (Lin et al., 2025); and (iii) *tool-augmented* LLM systems that pair a general LLM with external chemistry tools for planning, prediction, and validation, notably ChemCrow (Bran et al., 2023), SynAsk (Zhang et al., 2025a)). Beyond pure single-step generators, multimodal and route-context methods incorporate additional signals such as textual route context in RetroInText (Kang et al., 2025), while other lines explore using GP LLMs inside decision/search programs for synthesis planning and design, as in LLM-augmented decision programs (Wang et al., 2025; Liu et al., 2025).

In parallel, larger chemistry-focused LLMs and instruction-tuned checkpoints such as BatGPT-Chem (Yang et al., 2025), ChemLLM (Zhang et al., 2024), Mol-Instructions / LLaMA-MolInst adapters (Fang et al., 2024) aim to improve general chemical competence and controllability for downstream reaction tasks. Finally, emerging “reasoning-oriented” post-training directions target more structured chemical reasoning for retrosynthesis as seen in Chemma (Zhang et al., 2025c), atom-anchored LLM retrosynthesis (Hassen et al., 2025), and ether0 (Narayanan et al., 2025), attempting to improve decomposition/editing behavior without requiring additional chemistry-domain pretraining from scratch.

Benchmarking of LLMs. While several recent benchmarks evaluate LLMs on broad chemistry knowledge and reasoning (Guo et al., 2023; Runcie et al., 2026; Xu et al., 2025; Li et al., 2026; Song et al., 2025; Zhao et al., 2025a), they typically include general chemistry tasks, and few or no synthesis-planning tasks and therefore only indirectly reflect retrosynthetic capability.

3. Approach

The vast majority of SSRS benchmarks are based on the USPTO-50K test set (Maziarz et al., 2025; Torren-Peraire et al., 2024; Segler et al., 2018; Schwaller et al., 2020). This set consists of ~ 5K pairs of products and corresponding reactant(s), with each product typically having only one unique set of reactants. Any predicted reactants set that does not fully match the provided answers would be considered incorrect and the respective Top-K accuracy values will go down. This approach completely disregards the actual practice of SSRS, in which multiple plausible options for synthesizing a compound in the next-step reaction can be considered. For the vast majority of compounds, especially complex ones, there are decisively more than one way to synthesize them (see example at [Appendix C](#)). Undoubtedly, having a reaction exactly matching the reported example is a great fortune for a chemist. However, in most cases, because of the dispersed nature of chemical reaction space, when designing a retrosynthetic route, a chemist operates with more general concepts of reaction centers’ and functional groups’ intercompatibility, making a few steps of abstraction from exact matches. Here, to tackle the drawbacks of the previous “single ground-truth” paradigm, we propose ChemCensor, a new data-driven framework to score reactions based on the extraction of reaction centers and functional groups and their eigenprecedents and intercompatibility precedents analysis. By design, the framework mimics the way how a synthetic chemist evaluates a potential reaction to be included in the retrosynthetic route within search in chemical expert databases (Elsevier; [Chemical Abstracts Service \(CAS\)](#)). ChemCensor is a part of a larger benchmarking system **URSA** (**Utilitarian RetroSynthesis Assessment**), which is designed to score not only outputs from SSRS models, but also end-to-end retrosynthesis solutions and to be reported in detail separately.

3.1. ChemCensor Metric

ChemCensor is a precedent-based, quantitative metric for measuring *chemical plausibility* ([Figure 2](#)). For each reaction, the algorithm extracts its reaction center (**RC**, what bonds/atoms change) and the “static” functional-group (**FG**) context (which FGs remain present but are not transformed). The algorithm then checks whether the RCs and FGs have been observed in a relational database of reported reactions. The output (**ChemCensor Score**) is an integer confidence level (0–5) that directly reflects how well the step is supported by documented *synthetic precedents*. The higher CC values correspond to the broader substructural context of RC that can be matched to the actual synthetic precedent. In practical terms, ChemCensor answers a simple question: “*Have chemists successfully done this type of transformation before, and in the presence of these FGs?*” If yes, the reaction receives a higher score; if the synthetic precedents

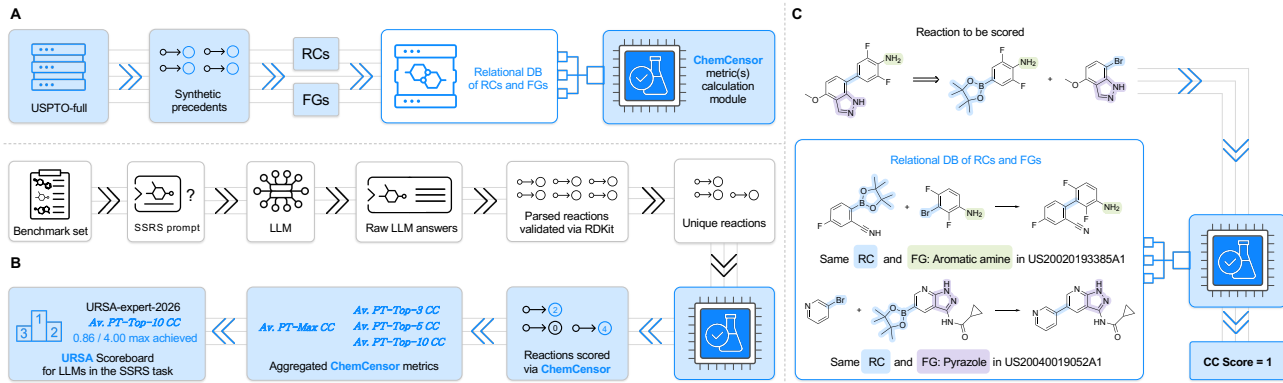


Figure 2. ChemCensor part of the URSA benchmark. **A.** The procedure of retrieval and chemistry-aware knowledge aggregation from **USPTO-full** into the relational DB of RCs and FGs. **B.** The pipeline of LLMs benchmarking for the SSRS task. **C.** The example of RC and FGs intercompatibility assessment during single reaction scoring within ChemCensor.

match only a topologically limited substructural context of RC, the score is low; if the algorithm cannot find supporting precedents for the RC and/or its FGs environment, the score is zero. The scoring procedure follows four steps:

1. **Split “what reacts” (RC) vs “what must be tolerated” (FGs).** The reaction is decomposed into (i) a hierarchical RC representation and (ii) a FG signature for the non-participating parts of the structures.
2. **Look up precedents for the RC.** The extracted RC patterns are matched against a precomputed library built from a reference dataset of confirmed reactions.
3. **Verify FGs compatibility.** The system checks whether the FGs present in the proposed step are compatible with that reaction center, based on FGs signatures aggregated from precedent examples.
4. **Assign a confidence level (CC Score).**

In this work, we distinguish five levels of reaction center annotation, denoted RC1, RC2, RC3, RC4 and RC5 corresponding to confidence levels and ChemCensor Scores from 1 to 5, respectively. The confidence level number provides the knowledge of the substructural context size of RC supported within synthetic precedents and FGs (N=515) compatibility precedents at this RC substructural context size. The smaller RC context size might be more popular in the reference dataset, but possesses low confidence. Oppositely, a larger RC context size provides greater confidence, but obviously is less represented in the reference set, especially considering the common context of non-reacting FGs. The details on how RC1-5 and FGs are organized are provided in [Appendix D](#).

ChemCensor knowledge base is grounded on the best-to-date publicly available **USPTO-full** dataset covering reactions from the US Patents from 1976 to 2016 ([Lowe, 2017](#)).

3.2. Benchmarking Sets

To evaluate the SSRS task outputs from LLMs, we proposed a new dataset, **URSA-expert-2026**. It is a benchmark dataset consisting of 100 synthetically plausible, machine-generated target molecules. They were generated within the generative chemistry pipeline ([Ivanenkov et al., 2023](#)) as potential inhibitors of novel drug targets ([Avram et al., 2021; 2022; 2023](#)). The synthetic accessibility status of these molecular structures is confirmed by expert synthetic chemists, who provided validated theoretical synthetic schemes (see example in [Appendix K](#)) supported by relevant references for reactions and leading to the curated CABBs (*commercially available building blocks*). All molecular structures in this dataset are novel and non-overlapping with publicly available reaction datasets, ensuring that they have not been used for training retrosynthesis models.

The URSA-expert-2026 set is intended as a primary benchmarking set for evaluating generalization, robustness, and exploratory capabilities of SSRS and MSRS models under conditions free from training-set memorization or data leakage.

We additionally report results on the widely adopted **USPTO-50K-test** ([Liu et al., 2017](#)) to ensure direct comparability with prior SSRS literature. For consistency with our evaluation protocol and to improve experimental reliability, we use a curated version of USPTO-50K-test, removing a small subset of reactions according to criteria described in [Appendix J](#). This dual-benchmark setup (URSA-expert-2026 as the main generalization benchmark and USPTO-50K-test as the community-standard reference) enables evaluation both on a leakage-resistant target pool and on an established baseline used across SSRS studies.

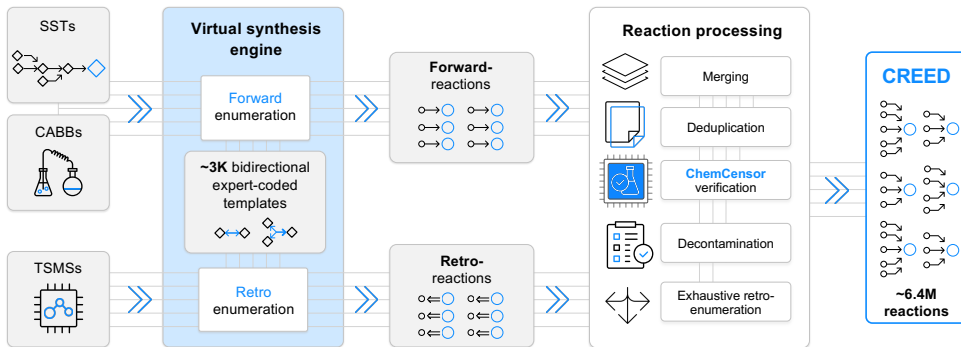


Figure 3. CREED (Comprehensive Reactant Exhaustive Enumeration Dataset) design process.

3.3. Aggregated Metrics

We used ChemCensor Score (CC) as an evaluation metric for a primary reaction.

As integral metrics for this benchmarking, we implemented additional metrics: **Av. PT-Max CC** and **Av. PT-Top-K**:

Av. PT-Max CC is calculated as the average of the Max CC values over all target molecules t in the benchmark set of size N , where Max CC for a target denotes the highest CC value among all CC scores obtained for the set of possible retro-reactions \mathcal{R}_t predicted for that target by a model:

$$\text{Max CC}(t) = \max_{r \in \mathcal{R}_t} \text{CC}(t, r) \quad (1)$$

$$\text{Av. PT-Max CC} = \frac{1}{N} \sum_{t=1}^N \text{Max CC}(t) \quad (2)$$

Av. PT-Top-K is calculated as the average of CC@K(t) over all target molecules in the benchmark dataset of size N , where CC@K(t) is the mean CC score across the Top- K *unique* predicted retro-reactions for target molecule t . To explicitly account for prediction diversity, the ranked list of model outputs is first *deduplicated* (exact duplicates are removed). If, after deduplication, fewer than K unique predictions remain, the missing slots are padded with zeros. This prevents artificially inflating the metric by repeating the same high-scoring prediction multiple times.

$$\text{CC}@K(t) = \frac{1}{K} \sum_{k=1}^K \text{CC}(t, r_{t,k}^{\text{uniq}}) \quad (3)$$

$$\text{Av. PT-Top-K} = \frac{1}{N} \sum_{t=1}^N \text{CC}@K(t) \quad (4)$$

3.4. CREED

In this work, we also introduce **CREED** (Comprehensive Reactant Exhaustive Enumeration Dataset), a large-scale and quality-controlled dataset of chemical reactions. CREED was built using two generation paradigms supported by an in-house virtual synthesis engine and the CC verification framework (see Fig. 3). First, in a forward route-generation regime, we performed construction of multistep synthetic pathways using the forward synthesis engine fueled with 1) $\sim 3K$ expert-coded bidirectional reaction templates, 2) CABBS as *starting materials* and 3) synthetic scheme templates (SSTs) derived from real-world syntheses of approved drugs (e.g., (Flick et al., 2022)). Individual elementary reactions were then extracted from the forward-generated routes. This approach covered $\sim 67\%$ of reaction templates. The remaining $\sim 33\%$ templates are not covered within drug-aware SSTs. Thus, we had to generate plausible template-specific molecular structures (TSMSS), which could be applied to the remaining templates in the retro-regime. After generating such molecular structures using the generative chemistry approach (Ivanenkov et al., 2023), the remaining templates were applied to them; and the resulting retro-reactions covered the missing templates. Afterwards, both the retro-reactions and forward-reactions were merged. All candidate reactions were subsequently verified with CC, and only those with CC Score > 0 were retained. After this quality-control step and decontamination against the USPTO-50K-test set, CREED comprises 6,382,667 unique reactions with theoretically supported plausibility by the CC module for 653,567 unique products.

CREED is designed to prioritize *chemical plausibility* over “single-ground-truth” convention. Multiple plausible reaction options for a single product are provided to enable diverse plausible SSRS model outputs, contrastingly to the USPTO-full, which mostly contains a single set of reactants per product. See such examples of MA (Multiple Answer) options and other details of CREED in Appendix G.

4. Experiments

In this section, we conduct an evaluation of recent foundation models and chemical specialists on the proposed ChemCensor benchmark to investigate the capabilities of these models in the Single Step Retrosynthesis task. Moreover, we train a novel **C3LM** (Chemistry Constraint–Consistent Language Model) on the proposed CREED and using ChemCensor metric as reward and show that carefully curated train corpora can substantially improve LM performance on the SSRS task. Additional training, resource, optimization, and other details can be found in [Appendix H](#).

4.1. Baseline Models

As baselines for our ChemCensor benchmark, we adopt the set of proprietary and open-weight language models. Our selection is focused on (i) widely accessible general-purpose language models and (ii) recent language models with general chemistry or retrosynthesis knowledge, specifically:

Proprietary Foundation Models: Grok 4.1 [2025](#); Gemini 2.5 Flash [2025a](#) and 3 Flash preview [2025b](#); GPT 5.1 [2025a](#) and 5.2 [2025b](#); Claude 4.5 Sonnet [2025b](#) and 4.5 Opus [2025a](#).

Open-weight Foundation Models: DeepSeek 3.2 [2025](#); Qwen 3 [2025d](#) and Kimi K2 [2025c](#).

Open-weight Chemical Specialist Models: ether0 [2025](#); NatureLM [2025](#) and RetroDFM-R [2025b](#).

4.2. C3LM Supervised Fine-Tuning

Training setups: Supervised Fine-Tuning (SFT) of C3LM model is performed in three variants, varying (i) the training data and (ii) whether the model is trained to produce reasoning. For training data, we use either CREED alone or concatenate it with a decontaminated USPTO-full ([Lowe, 2017](#)), which is upsampled to match the CREED size.

Stage 1 (no reasoning). We initialize C3LM model with Qwen3-8B checkpoint [2025d](#) and train *without reasoning* for 40,000 steps: (i) *no-reasoning* C3LM trained on CREED, and (ii) *no-reasoning* C3LM trained on CREED+USPTO-full.

Stage 2 (with reasoning). Next, starting from stage-1 CREED+USPTO-full model checkpoint, we continue SFT with reasoning traces for an additional 40,000 steps, yielding (iii) C3LM *with reasoning*.

Training procedure: On each training step, we utilize a total 524,288 tokens context windows across all GPUs and pack ([Brown et al., 2020b](#)) multiple training sequences into each GPU available context window.

Training Data Preprocessing: Similarly to other chemical

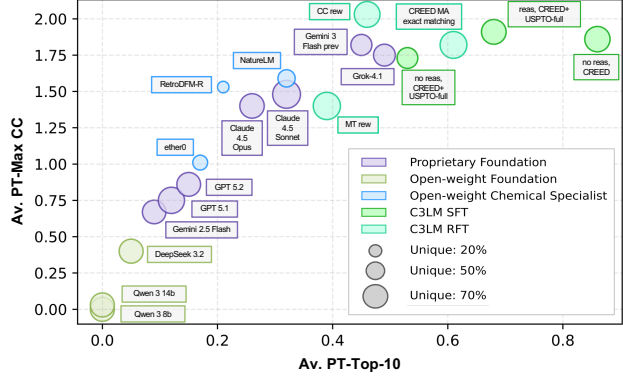


Figure 4. LLMs' performance on URSA-expert-2026 set.

language models ([Livne et al., 2024](#); [Pei et al., 2023](#)), we extend the base vocabulary with SMILES format ([Weininger, 1988](#)) specific tokens; this is aimed at isolating chemical tokens from natural-language tokens and providing a consistent representation of SMILES entities. During the training, we tokenize SMILES into specialised tokens always in model outputs, and with 0.5 probability for user input; we adopt this strategy to align Qwen3 base checkpoint chemical knowledge and new tokens. To improve chemical generalisation, we augment SMILES entities during training by applying non-canonical random traversal. Examples of training prompts can be found in [Appendix I](#).

4.3. C3LM Reinforcement Learning Fine-Tuning

Training procedure: Online Reinforcement Learning Fine-Tuning (RFT) of the *no-reasoning* C3LM (CREED+USPTO-full) model was performed using single-reward Group Relative Policy Optimization (GRPO) ([Shao et al., 2024](#)). RFT used the same CREED training split as SFT with a GRPO group size of 16. Each reward function assigns a reward in the range $(-1, +1)$.

ChemCensor Reward: Applies the confidence level of ChemCensor as a reward. For a generated reaction, the reward is the chemical plausibility between $0 - 5$, scaled to $(0, +1)$. A reward of -1 is assigned when the generated reactant SMILES is invalid.

CREED Multiple Answer (MA) Exact Matching: Applies a binary reward of $+1$ if the generated reactants exists in the exhaustive enumerated list of CREED and -1 if not.

Molecular Transformer Reward: Applies a binary reward based on agreement with Molecular Transformer (MT) ([Schwaller et al., 2019a](#)). The generated reactants from our model are passed to MT and a score of $+1$ is assigned if the MT-predicted product matches the original input to our model and -1 if not. MT was used as the forward synthesis reward function in ether0 ([Narayanan et al., 2025](#)) and the

Model	URSA-expert-2026					USPTO-50K-test				
	Unique	Max	Av. PT-Top-K CC @3	Av. PT-Top-K CC @5	Av. PT-Top-K CC @10	Unique	Max	Av. PT-Top-K CC @3	Av. PT-Top-K CC @5	Av. PT-Top-K CC @10
<i>Proprietary Foundation Models</i>										
Grok-4.1	43%	1.75	1.30	0.93	0.49	—	—	—	—	—
Gemini 2.5 Flash	50%	0.67	0.30	0.18	0.09	—	—	—	—	—
Gemini 3 Flash preview	40%	1.82	1.27	0.89	0.45	—	—	—	—	—
GPT 5.1	62%	0.75	0.36	0.23	0.12	59%	1.55	0.72	0.45	0.23
GPT 5.2	51%	0.86	0.48	0.29	0.15	52%	2.05	1.01	0.63	0.32
Claude 4.5 Sonnet	70%	1.48	0.95	0.64	0.32	<u>56%</u>	3.38	1.82	1.16	0.59
Claude 4.5 Opus	54%	1.40	0.81	0.51	0.26	44%	3.32	1.64	1.02	0.51
<i>Open-weight Foundation Models</i>										
DeepSeek 3.2	52%	0.40	0.16	0.10	0.05	55%	1.14	0.46	0.28	0.14
Qwen3 8b	52%	0.00	0.00	0.00	0.00	55%	0.05	0.03	0.02	0.01
Qwen3 14b	52%	0.03	0.01	0.00	0.00	54%	0.10	0.03	0.02	0.01
Kimi K2	0%	0.00	0.00	0.00	0.00	0%	0.04	0.01	0.01	0.00
<i>Open-weight Chemical Specialist Models</i>										
ether0	20%	1.01	0.55	0.35	0.17	19%	2.08	1.07	0.67	0.34
NatureLM	27%	1.59	0.99	0.63	0.32	20%	3.99	1.86	1.15	0.58
RetroDFM-R	12%	1.53	0.70	0.43	0.21	8%	4.36	1.56	0.94	0.47
<i>C3LM, Supervised Fine-Tuning</i>										
No reas. (CREED only)	58%	<u>1.86</u>	<u>1.51</u>	1.29	0.86	46%	3.10	2.12	<u>1.64</u>	0.95
No reas. (CREED+USPTO-full)	39%	1.73	1.23	0.90	0.53	25%	4.09	<u>2.00</u>	1.27	0.65
With reas.	55%	1.91	1.52	<u>1.21</u>	<u>0.68</u>	40%	<u>4.27</u>	2.52	1.69	0.86
<i>C3LM, Reinforcement Learning Fine-Tuning</i>										
ChemCensor reward	60%	2.03	1.35	0.89	0.46	59%	3.98	1.96	1.23	0.62
CREED MA exact-matching	<u>65%</u>	1.82	1.45	1.13	0.61	59%	2.98	1.89	1.32	0.67
MolTransformer reward	67%	1.40	1.00	0.73	0.39	55%	3.43	1.71	1.08	0.54

Table 1. Single-step retrosynthesis baselines on plausibility-based evaluation. **Unique**: fraction of unique valid reactant sets among samples. **Max**: per-target maximum ChemCensor score averaged over targets. **Av. PT-Top-K CC**: per-target average ChemCensor score over top-K unique predictions. We highlight best values with **bold** and second best with underline.

same underlying model weights were used (MT trained to 40,000 steps on USPTO480K (Jin et al., 2017)).

4.4. Evaluation Protocol

We perform a benchmark of all models from Sec. 4.1 and proposed C3LM model on the proposed URSA-expert-2026 and revised USPTO-50K-test sets. For each test sets product, we generate 15 independent responses from each model.

All models were evaluated without external tools (no code execution or internet use) to isolate the core model capability. Reasoning was enabled in all models that support it with the default reasoning budget. We used a few-shot prompting method with five examples. The examples were chosen from the training set of the USPTO-full dataset at random for each data item in the test sets. The queries in the few-shot

examples and the final question were sampled at random from a set of templates provided in the Appendix I. For models released with task-specific retrosynthesis prompts by their authors, we used those prompts instead.

We do not report USPTO-50K-test results for Grok-4.1, Gemini 2.5 Flash and Gemini 3 Flash preview, because API request limits and/or long generation times prevented us from obtaining the full set of required completions on this larger dataset with 15 repetitions per example to reliably estimate the proposed metrics. Our proposed URSA-expert-2026 benchmark is a more reliable estimate of the generalizability of such LLMs that are usually prone to USPTO-50K-test set contamination.

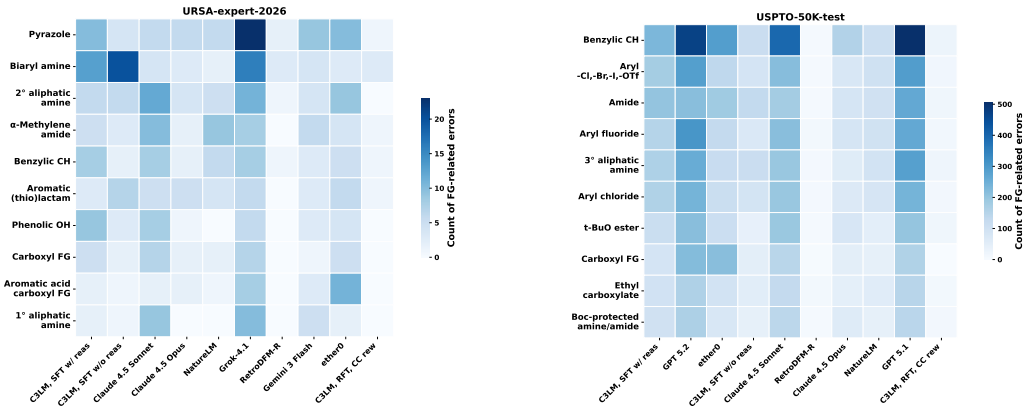


Figure 5. FG-related error profiles across models on test sets. The heat map shows the count of CC FG incompatibility errors across the best 10 models by Av. PT-Top-10 CC (see Table 1), darker cells indicate a higher error number. See FGs in Appendix F.

5. Main Findings and Discussion

Table 1 reports ChemCensor performance across all models. Another results representation is given as scatter plots in Figure 4 and Appendix A. Overall, the majority of *Proprietary Foundation* and *Open-weight Chemical Specialist* language models generate a large fraction of valid and unique reactants and achieve strong ChemCensor scores on the USPTO-50K-test split. However, URSA-expert-2026 appears to be a considerably harder setting: performance drops sharply for nearly all models. Surprisingly, *Open-Weight Foundation* language models (with the exception of DeepSeek) tend to perform markedly worse: several models fail to produce valid and/or unique reactants, and even when they do, their predictions often receive low CC scores.

Another view on models’ performance is provided in Figure 1 to highlight the differentiation in output reactions diversity across the models rather than CC values and to show the mechanics of CC-based evaluation. While red bars report the reactions failed to align any *synthetic precedent*, yellow ones show those with plausible RC, but failed the RC/FGs intercompatibility check. The usage of CREED for LLMs training is proven for both diverse (low grey bars) and plausible (high green bars) reactions outcome. Interestingly, the models differently fail to satisfy RC/FGs intercompatibility criteria. As the heat map at Figure 5 shows, some models can self-confidently oversample reactions failing to handle aryl halides, various amines and other FGs selectively.

We further show that training on the proposed large, high-quality CREED enables models to outperform all baseline models. In particular, our C3LM, initialized from the Qwen3 8B checkpoint, which has one of the lowest baseline CC scores, achieves the best or second-best CC results on both URSA-expert-2026 and USPTO-50K-test after SFT and RFT. The only exception is RetroDFM-R on USPTO-50K-test, which attains the highest per-target maximum

ChemCensor score despite low validity and uniqueness. Results indicate that SFT with reasoning improves PT-Max CC compared to SFT without reasoning. Adding USPTO-full to training unexpectedly reduces uniqueness, although it boosts performance on USPTO-50K-test.

RFT with the ChemCensor reward increases PT-Max CC on URSA-expert-2026, but improvements shrink as Top-K grows (suggesting reduced diversity), whereas exact-match RFT yields smaller PT-Max CC gains but more consistent Top-K improvements. By contrast, Molecular-Transformer-reward RFT degrades performance on URSA-expert-2026 (while harming USPTO-50K-test less), likely because the reward model is trained only on USPTO chemistry and generalizes poorly out of domain. Important to say, that RFT CC model shows the best performance from the perspective of satisfying RCs and FGs intercompatibility that can be noticed from its narrowest yellow bar Figure 1 and the corresponding light colored column at the heat-map Figure 5, suggesting the model indirectly learned the concepts of chemoselectivity and regioselectivity.

6. Conclusion

We propose ChemCensor, a plausibility-based metric for single-step retrosynthesis that evaluates synthetic precedent and key chemical constraints beyond exact-match Top-K accuracy. Using it, we construct CREED ($\sim 6.4M$ verified reactions) and release URSA-expert-2026, an expert-annotated out-of-domain benchmark of 100 novel targets.

Benchmarking a broad set of LMs shows that performance on the USPTO-50K-test does not reliably transfer to URSA-expert-2026, which is substantially harder. Fine-tuning on CREED is highly effective: proposed C3LM model achieves best or second-best ChemCensor scores on both benchmarks, outperforming general-purpose foundation and chemical specialist baselines.

Impact Statement

This paper proposes ChemCensor, an evaluation metric and benchmarking protocol for single-step retrosynthesis, and introduces supporting datasets and models. If adopted, these tools could improve the reliability and reproducibility of research claims in computer-aided synthesis planning and help practitioners compare systems in a way that better reflects chemical plausibility. In the drug-discovery setting, more faithful evaluation reduces wasted effort on implausible routes and accelerates iteration by prioritizing synthetically feasible designs.

Potential negative impacts stem from dual use. Improved retrosynthesis models and benchmarking may potentially lower barriers to designing synthesis routes for harmful or controlled substances, and they may enable misuse if deployed without safeguards. The suggested CREED was filtered by medicinal chemistry patterns and decontaminated to alleviate such risks, with the only focus on safe drug-like molecules as opposed to harmful substances.

We also mitigate such risks by focusing the contribution on evaluation methodology, emphasizing out-of-domain and plausibility-aware assessment rather than providing an end-to-end automated synthesis capability, and by documenting dataset construction, decontamination, and limitations to support responsible use. We encourage future work to incorporate access controls and misuse-aware filtering when applying the resulting models in high-risk settings, and to audit benchmark coverage and biases as reaction data and model capabilities evolve.

References

Anthropic. System card: Claude opus 4.5, November 2025a. URL <https://www.anthropic.com/clause-opus-4-5-system-card>.

Anthropic. System card: Claude sonnet 4.5, September 2025b. URL <https://www.anthropic.com/clause-sonnet-4-5-system-card>.

Avram, S., Halip, L., Curpan, R., and Oprea, T. I. Novel drug targets in 2020. *Nat. Rev. Drug Discov.*, 20(5):333, May 2021. doi: 10.1038/d41573-021-00057-z. URL <https://www.nature.com/articles/d41573-021-00057-z>.

Avram, S., Halip, L., Curpan, R., and Oprea, T. I. Novel drug targets in 2021. *Nat. Rev. Drug Discov.*, 21(5):328, May 2022. doi: 10.1038/d41573-022-00057-7. URL <https://www.nature.com/articles/d41573-022-00057-7>.

Avram, S., Halip, L., Curpan, R., and Oprea, T. I. Novel drug targets in 2022. *Nat. Rev. Drug Discov.*, 22(6):437, June 2023. doi: 10.1038/d41573-023-00068-y. URL <https://www.nature.com/articles/d41573-023-00068-y>.

Bran, A. M., Cox, S., Schilter, O., Baldassari, C., White, A. D., and Schwaller, P. ChemCrow: Augmenting large-language models with chemistry tools. *arXiv [physics.chem-ph]*, April 2023. doi: 10.48550/arXiv.2304.05376. URL <http://arxiv.org/abs/2304.05376>.

Brown, T., Mann, B., Ryder, N., Subbiah, M., Kaplan, J. D., Dhariwal, P., Neelakantan, A., Shyam, P., Sastry, G., Askell, A., Agarwal, S., Herbert-Voss, A., Krueger, G., Henighan, T., Child, R., Ramesh, A., Ziegler, D., Wu, J., Winter, C., Hesse, C., Chen, M., Sigler, E., Litwin, M., Gray, S., Chess, B., Clark, J., Berner, C., McCandlish, S., Radford, A., Sutskever, I., and Amodei, D. Language models are few-shot learners. In Larochelle, H., Ranzato, M., Hadsell, R., Balcan, M., and Lin, H. (eds.), *Advances in Neural Information Processing Systems*, volume 33, pp. 1877–1901. Curran Associates, Inc., 2020a. URL https://proceedings.neurips.cc/paper_files/paper/2020/file/1457c0d6bfcb4967418bfb8ac142f64a-Paper.pdf.

Brown, T., Mann, B., Ryder, N., Subbiah, M., Kaplan, J. D., Dhariwal, P., Neelakantan, A., Shyam, P., Sastry, G., Askell, A., Agarwal, S., Herbert-Voss, A., Krueger, G., Henighan, T., Child, R., Ramesh, A., Ziegler, D., Wu, J., Winter, C., Hesse, C., Chen, M., Sigler, E., Litwin, M., Gray, S., Chess, B., Clark, J., Berner, C., McCandlish, S., Radford, A., Sutskever, I., and Amodei, D. Language models are few-shot learners. In Larochelle, H., Ranzato, M., Hadsell, R., Balcan, M., and Lin, H. (eds.), *Advances in Neural Information Processing Systems*, volume 33, pp. 1877–1901. Curran Associates, Inc., 2020b. URL https://proceedings.neurips.cc/paper_files/paper/2020/file/1457c0d6bfcb4967418bfb8ac142f64a-Paper.pdf.

Chemical Abstracts Service (CAS). SciFinder – retrosynthesis software. URL <https://www.cas.org/solutions/cas-scifinder-discovery-platform/cas-scifinder/synthesis-planning>. Accessed: 2026-01-20.

Chen, S. and Jung, Y. Deep retrosynthetic reaction prediction using local reactivity and global attention. *JACS Au*, 1(10):1612–1620, 2021. doi: 10.1021/jacsau.1c00246. URL <https://doi.org/10.1021/jacsau.1c00246>. PMID: 34723264.

Choe, J., Kim, H., Chok, Y. T., Gim, M., and Kang, J. Retrosynthetic crosstalk between single-step reaction and multi-step planning. *J. Cheminform.*, 17(1):130, August 2025. doi: 10.1186/s13321-025-01088-z. URL <https://link.springer.com/article/10.1186/s13321-025-01088-z>.

Corey, E. J. General methods for the construction of complex molecules. *Pure and Applied Chemistry*, 14(1):19–38, 1967. doi: doi:10.1351/pac196714010019. URL <https://www.degruyterbrill.com/document/doi/10.1351/pac196714010019/html>.

Daylight Chemical Information Systems, I. SMARTS — a language for describing molecular patterns, 2007. URL <https://www.daylight.com/dayhtml/doc/theory/theory.smarts.html>.

DeepSeek-AI. Deepseek-v3.2: Pushing the frontier of open large language models, 2025. URL <https://arxiv.org/abs/2512.02556>.

Deng, Y., Zhao, X., Sun, H., Chen, Y., Wang, X., Xue, X., Li, L., Song, J., Hsieh, C.-Y., Hou, T., Pan, X., Alomar, T. S., Ji, X., and Wang, X. RS-GPT: a generative transformer model for retrosynthesis planning pre-trained on ten billion datapoints. *Nat. Commun.*, 16(1):7012, July 2025. doi: 10.1038/s41467-025-62308-6. URL <https://www.nature.com/articles/s41467-025-62308-6>.

Ehrt, C., Krause, B., Schmidt, R., Ehmki, E. S. R., and Rarey, M. Smarts.plus – a toolbox for chemical pattern design. *Molecular Informatics*, 39(12):e2000216, 2020. doi: 10.1002/minf.202000216. URL <https://doi.org/10.1002/minf.202000216>.

Elsevier. Reaxys. URL <https://www.elsevier.com/solutions/reaxys>. Accessed: 2026-01-20.

Fang, Y., Liang, X., Zhang, N., Liu, K., Huang, R., Chen, Z., Fan, X., and Chen, H. Mol-instructions: A large-scale biomolecular instruction dataset for large language models, 2024. URL <https://arxiv.org/abs/2306.08018>.

Flick, A. C., Leverett, C. A., Ding, H. X., McInturff, E. L., Fink, S. J., Mahapatra, S., Carney, D. W., Lindsey, E. A., DeForest, J. C., France, S. P., Berritt, S., Bigi-Botterill, S. V., Gibson, T. S., Watson, R. B., Liu, Y., and O'Donnell, C. J. Synthetic approaches to the new drugs approved during 2020. *J. Med. Chem.*, 65(14):9607–9661, July 2022. doi: 10.1021/acs.jmedchem.2c00710. URL <https://pubs.acs.org/doi/10.1021/acs.jmedchem.2c00710>.

Gao, W. and Coley, C. W. The synthesizability of molecules proposed by generative models. *Journal of Chemical Information and Modeling*, 60(12):5714–5723, 2020. doi: 10.1021/acs.jcim.0c00174. URL <https://doi.org/10.1021/acs.jcim.0c00174>.

Grzybowski, B. A., Szymkuć, S., Gajewska, E. P., Molga, K., Dittwald, P., Wołos, A., and Klucznik, T. Chematica: A story of computer code that started to think like a chemist. *Chem.*, 4(3):390–398, 2018. ISSN 2451-9294. doi: <https://doi.org/10.1016/j.chempr.2018.02.024>. URL <https://www.sciencedirect.com/science/article/pii/S2451929418300858>.

Guo, T., Guo, K., Nan, B., Liang, Z., Guo, Z., Chawla, N. V., Wiest, O., and Zhang, X. What can large language models do in chemistry? a comprehensive benchmark on eight tasks. In *Proceedings of the 37th International Conference on Neural Information Processing Systems*, NIPS '23, Red Hook, NY, USA, 2023. Curran Associates Inc. URL https://proceedings.neurips.cc/paper_files/paper/2023/file/bbb330189ce02be00cf7346167028ab1-Paper-Datasets_and_Benchmarks.pdf.

Hassen, A. K., Bernatavicius, A., Janssen, A. P. A., Preuss, M., van Westen, G. J. P., and Clevert, D.-A. Atom-anchored llms speak chemistry: A retrosynthesis demonstration, 2025. URL <https://arxiv.org/abs/2510.16590>.

Hastedt, F., Bailey, R. M., Hellgardt, K., Yaliraki, S. N., del Rio Chanona, E. A., and Zhang, D. Investigating the reliability and interpretability of machine learning frameworks for chemical retrosynthesis. *Digit. Discov.*, 3(6):1194–1212, 2024. doi: 10.1039/d4dd00007b. URL <https://pubs.rsc.org/en/content/articlehtml/2024/dd/d4dd00007b>.

Ivanenkov, Y. A., Polykovskiy, D., Bezrukov, D., Zagribelnyy, B., Aladinskiy, V., Kamya, P., Aliper, A., Ren, F., and Zhavoronkov, A. Chemistry42: An AI-driven platform for molecular design and optimization. *J. Chem. Inf. Model.*, 63(3):695–701, February 2023. doi: 10.1021/acs.jcim.2c01191. URL <https://pubs.acs.org/doi/abs/10.1021/acs.jcim.2c01191>.

Jiang, Y., Yu, Y., Kong, M., Mei, Y., Yuan, L., Huang, Z., Kuang, K., Wang, Z., Yao, H., Zou, J., Coley, C. W., and Wei, Y. Artificial intelligence for retrosynthesis prediction. *Engineering*, 25:32–50, 2023. ISSN 2095-8099. doi: <https://doi.org/10.1016/j.eng.2022.04.021>. URL <https://www.sciencedirect.com/science/article/pii/S2095809922005665>.

Jin, W., Coley, C., Barzilay, R., and Jaakkola, T. Predicting organic reaction outcomes with weisfeiler-lehman

network. In Guyon, I., Luxburg, U. V., Bengio, S., Wallach, H., Fergus, R., Vishwanathan, S., and Garnett, R. (eds.), *Advances in Neural Information Processing Systems*, volume 30. Curran Associates, Inc., 2017. URL https://proceedings.neurips.cc/paper_files/paper/2017/file/ced556cd9f9c0c8315cfbe0744a3baf0-Paper.pdf.

Kang, C., Liu, X., and Guo, F. Retrioutext: A multimodal large language model enhanced framework for retrosynthetic planning via in-context representation learning. In *The Thirteenth International Conference on Learning Representations*, 2025. URL <https://openreview.net/forum?id=J6e4hurEKd>.

Levenshtein, V. I. Binary codes capable of correcting deletions, insertions and reversals. *Soviet Physics Doklady*, 10:707–710, 1966. URL <https://nymity.ch/sybilhunting/pdf/Levenshtein1966a.pdf>.

Li, H., Fang, X., Li, Y., Huang, C., Wang, J., Wang, X., Bai, H., Hao, B., Lin, S., Liang, H., Zhang, L., and Ke, G. Rxnbench: A multimodal benchmark for evaluating large language models on chemical reaction understanding from scientific literature, 2026. URL <https://arxiv.org/abs/2512.23565>.

Lin, J. Divergence measures based on the shannon entropy. *IEEE Transactions on Information Theory*, 37(1):145–151, 1991. doi: 10.1109/18.61115. URL <https://ieeexplore.ieee.org/document/61115>.

Lin, X., Liu, Q., Xiang, H., Zeng, D., and Zeng, X. Enhancing chemical reaction and retrosynthesis prediction with large language model and dual-task learning. In *Proceedings of the Thirty-Fourth International Joint Conference on Artificial Intelligence, IJCAI '25*, 2025. ISBN 978-1-956792-06-5. doi: 10.24963/ijcai.2025/840. URL <https://doi.org/10.24963/ijcai.2025/840>.

Liu, B., Ramsundar, B., Kawthekar, P., Shi, J., Gomes, J., Luu Nguyen, Q., Ho, S., Sloane, J., Wender, P., and Pande, V. Retrosynthetic reaction prediction using neural sequence-to-sequence models. *ACS Central Science*, 3(10):1103–1113, 2017. doi: 10.1021/acscentsci.7b00303. URL <https://doi.org/10.1021/acscentsci.7b00303>. PMID: 29104927.

Liu, S., Tu, Z., Xu, M., Zhang, Z., Lin, L., Ying, R., Tang, J., Zhao, P., and Wu, D. Fusionretro: Molecule representation fusion via in-context learning for retrosynthetic planning. In *Proceedings of the 40th International Conference on Machine Learning*, volume 202 of *Proceedings of Machine Learning Research*, pp. 22028–22041. PMLR, 2023. URL <https://proceedings.mlr.press/v202/liu23ah.html>.

Liu, W., Feng, J., Yu, H., Song, Y., Li, Y., Zhang, S., BAI, L., Ma, W.-Y., and Zhou, H. Retro-r1: LLM-based agentic retrosynthesis. In *The Thirty-ninth Annual Conference on Neural Information Processing Systems*, 2025. URL <https://openreview.net/forum?id=30iBKSQMXn>.

Livne, M., Miftahutdinov, Z., Tutubalina, E., Kuznetsov, M., Polykovskiy, D., Brundyn, A., Jhunjhunwala, A., Costa, A., Aliper, A., Aspuru-Guzik, A., and Zhavoronkov, A. nach0: multimodal natural and chemical languages foundation model. *Chem. Sci.*, 15:8380–8389, 2024. doi: 10.1039/D4SC00966E. URL <http://dx.doi.org/10.1039/D4SC00966E>.

Lowe, D. Chemical reactions from US patents (1976–Sep2016). 6 2017. doi: 10.6084/m9.figshare.5104873.v1. URL https://figshare.com/articles/dataset/Chemical_reactions_from_US_patents_1976-Sep2016_5104873.

Maziarz, K., Tripp, A., Liu, G., Stanley, M., Xie, S., Gaiński, P., Seidl, P., and Segler, M. H. S. Re-evaluating retrosynthesis algorithms with syntheseus. *Faraday Discuss.*, 256:568–586, 2025. doi: 10.1039/D4FD00093E. URL <http://dx.doi.org/10.1039/D4FD00093E>.

Morgunov, A. and Batista, V. S. Procrustean bed for ai-driven retrosynthesis: A unified framework for reproducible evaluation, 2025. URL <https://arxiv.org/abs/2512.07079>.

Narayanan, S. M., Braza, J. D., Griffiths, R.-R., Bou, A., Wellawatte, G., Ramos, M. C., Mitchener, L., Rodrigues, S. G., and White, A. D. Training a scientific reasoning model for chemistry, 2025. URL <https://arxiv.org/abs/2506.17238>.

OpenAI. Gpt-5.1 instant and gpt-5.1 thinking system card addendum, November 2025a. URL https://cdn.openai.com/pdf/4173ec8d-1229-47db-96de-06d87147e07e/5_1_system_card.pdf.

OpenAI. Update to gpt-5 system card: Gpt-5.2, December 2025b. URL https://cdn.openai.com/pdf/3a4153c8-c748-4b71-8e31-aecbde944f8d/oai_5_2_system-card.pdf.

Papineni, K., Roukos, S., Ward, T., and Zhu, W.-J. Bleu: a method for automatic evaluation of machine translation. In *Proceedings of the 40th Annual Meeting of the Association for Computational Linguistics*, pp. 311–318, 2002. doi: 10.3115/1073083.1073135. URL <https://aclanthology.org/P02-1040/>.

Pei, Q., Zhang, W., Zhu, J., Wu, K., Gao, K., Wu, L., Xia, Y., and Yan, R. BioT5: Enriching cross-modal integration in biology with chemical knowledge and natural language associations. In Bouamor, H., Pino, J., and Bali, K. (eds.), *Proceedings of the 2023 Conference on Empirical Methods in Natural Language Processing*, pp. 1102–1123, Singapore, December 2023. Association for Computational Linguistics. doi: 10.18653/v1/2023.emnlp-main.70. URL <https://aclanthology.org/2023.emnlp-main.70>.

Rasley, J., Rajbhandari, S., Ruwase, O., and He, Y. DeepSpeed: System optimizations enable training deep learning models with over 100 billion parameters. In *Proceedings of the 26th ACM SIGKDD International Conference on Knowledge Discovery & Data Mining*, KDD '20, pp. 3505–3506, New York, NY, USA, 2020. Association for Computing Machinery. ISBN 9781450379984. doi: 10.1145/3394486.3406703. URL <https://doi.org/10.1145/3394486.3406703>.

Runcie, N. T., Deane, C. M., and Imrie, F. Assessing the chemical intelligence of large language models. *J. Chem. Inf. Model.*, 66(1):216–227, January 2026. doi: 10.1021/acs.jcim.5c02145. URL <https://pubs.acs.org/doi/10.1021/acs.jcim.5c02145>.

Schwaller, P., Laino, T., Gaudin, T., Bolgar, P., Hunter, C. A., Bekas, C., and Lee, A. A. Molecular transformer: A model for uncertainty-calibrated chemical reaction prediction. *ACS Central Science*, 5(9):1572–1583, 2019a. doi: 10.1021/acscentsci.9b00576. URL <https://doi.org/10.1021/acscentsci.9b00576>. PMID: 31572784.

Schwaller, P., Petraglia, R., Zullo, V., Nair, V. H., Haeuselmann, R. A., Pisoni, R., Bekas, C., Iuliano, A., and Laino, T. Predicting retrosynthetic pathways using transformer-based models and a hyper-graph exploration strategy. *Chem. Sci.*, 11: 3316–3325, 2020. doi: 10.1039/C9SC05704H. URL <https://pubs.rsc.org/en/content/articlelanding/2020/sc/c9sc05704h>.

Schwaller, P. et al. Evaluation metrics for single-step retrosynthetic models. In *NeurIPS Workshop on Machine Learning and the Physical Sciences (ML4PS)*, 2019b. URL https://ml4physicalsciences.github.io/2019/files/NeurIPS_ML4PS_2019_116.pdf. Workshop paper.

Segler, M. H. S. and Waller, M. P. Neural-symbolic machine learning for retrosynthesis and reaction prediction. *Chemistry – A European Journal*, 23(25):5966–5971, 2017. doi: <https://doi.org/10.1002/chem.201605499>.

URL <https://chemistry-europe.onlinelibrary.wiley.com/doi/abs/10.1002/chem.201605499>.

Segler, M. H. S., Preuss, M., and Waller, M. P. Planning chemical syntheses with deep neural networks and symbolic AI. *Nature*, 555(7698):604–610, March 2018. doi: 10.1038/nature25978. URL <https://www.nature.com/articles/nature25978>.

Shao, Z., Wang, P., Zhu, Q., Xu, R., Song, J., Bi, X., Zhang, H., Zhang, M., Li, Y. K., Wu, Y., and Guo, D. Deepseekmath: Pushing the limits of mathematical reasoning in open language models, 2024. URL <https://arxiv.org/abs/2402.03300>.

Shee, Y., Morgunov, A., Li, H., and Batista, V. S. Directmultistep: Direct route generation for multistep retrosynthesis. *Journal of Chemical Information and Modeling*, 65(8):3903–3914, 2025. doi: 10.1021/acs.jcim.4c01982. URL <https://doi.org/10.1021/acs.jcim.4c01982>.

Song, Z., Lu, J., Du, Y., Yu, B., Pruyn, T. M., Huang, Y., Guo, K., Luo, X., Qu, Y., Qu, Y., Wang, Y., Wang, H., Guo, J., Gan, J., Shojaee, P., Luo, D., Bran, A. M., Li, G., Zhao, Q., Luo, S.-X. L., Zhang, Y., Zou, X., Zhao, W., Zhang, Y. F., Zhang, W., Zheng, S., Zhang, S., Khan, S. T., Rajabi-Kochi, M., Paradi-Maropakis, S., Baltoiu, T., Xie, F., Chen, T., Huang, K., Luo, W., Fang, M., Yang, X., Cheng, L., He, J., Hassoun, S., Zhang, X., Wang, W., Reddy, C. K., Zhang, C., Zheng, Z., Wang, M., Cong, L., Gomes, C. P., Hsieh, C.-Y., Nandy, A., Schwaller, P., Kulik, H. J., Jia, H., Sun, H., Moosavi, S. M., and Duan, C. Evaluating large language models in scientific discovery, 2025. URL <https://arxiv.org/abs/2512.15567>.

Team, G. 2.5 flash and native capabilities – audio & image model card, September 2025a. URL <https://storage.googleapis.com/deepmind-media/Model-Cards/Gemini-2-5-Flash-Model-Card.pdf>.

Team, G. Gemini 3 flash model card, December 2025b. URL <https://deepmind.google/models/model-cards/gemini-3-flash/>.

Team, K. Kimi K2: Open agentic intelligence, 2025c. URL <https://arxiv.org/abs/2507.20534>.

Team, Q. Qwen3 technical report, 2025d. URL <https://arxiv.org/abs/2505.09388>.

Tetko, I. V., Karpov, P., Van Deursen, R., and Godin, G. State-of-the-art augmented nlp transformer models for direct and single-step retrosynthesis. *Nature*

Communications, 11(1):5575, 2020. doi: 10.1038/s41467-020-19266-y. URL <https://www.nature.com/articles/s41467-020-19266-y>.

Torren-Peraire, P., Hassen, A. K., Genheden, S., Verhoeven, J., Clevert, D.-A., Preuss, M., and Tetko, I. V. Models matter: the impact of single-step retrosynthesis on synthesis planning. *Digital Discovery*, 3:558–572, 2024. doi: 10.1039/D3DD00252G. URL <http://dx.doi.org/10.1039/D3DD00252G>.

Tu, Z., Levin, I., and Coley, C. W. *Computer-Assisted Synthesis Planning*, chapter 11, pp. 423–459. John Wiley & Sons, Ltd, 2023. ISBN 9781119855668. doi: <https://doi.org/10.1002/9781119855668.ch11>. URL <https://onlinelibrary.wiley.com/doi/abs/10.1002/9781119855668.ch11>.

Vléduts, G. Concerning one system of classification and codification of organic reactions. *Information Storage and Retrieval*, 1(2):117–146, 1963. ISSN 0020-0271. doi: [https://doi.org/10.1016/0020-0271\(63\)90013-5](https://doi.org/10.1016/0020-0271(63)90013-5). URL <https://www.sciencedirect.com/science/article/pii/0020027163900135>.

Wang, H., Guo, J., Kong, L., Ramprasad, R., Schwaller, P., Du, Y., and Zhang, C. Llm-augmented chemical synthesis and design decision programs, 2025. URL <https://arxiv.org/abs/2505.07027>.

Weininger, D. SMILES, a chemical language and information system. 1. introduction to methodology and encoding rules. *Journal of Chemical Information and Computer Sciences*, 28(1):31–36, 1988. doi: 10.1021/ci00057a005. URL <https://doi.org/10.1021/ci00057a005>.

Westerlund, A. M., Sigmund, L. M., Kannas, C., Genheden, S., and Kabeshov, M. Toward lab-ready ai synthesis plans with protection strategies and route scoring. *ChemRxiv*, 2025(1031), 2025. doi: 10.26434/chemrxiv-2025-gdrr8. URL <https://chemrxiv.org/doi/abs/10.26434/chemrxiv-2025-gdrr8>.

Wolf, T., Debut, L., Sanh, V., Chaumond, J., Delangue, C., Moi, A., Cistac, P., Rault, T., Louf, R., Funtowicz, M., Davison, J., Shleifer, S., von Platen, P., Ma, C., Jernite, Y., Plu, J., Xu, C., Le Scao, T., Gugger, S., Drame, M., Lhoest, Q., and Rush, A. Transformers: State-of-the-art natural language processing. In Liu, Q. and Schlangen, D. (eds.), *Proceedings of the 2020 Conference on Empirical Methods in Natural Language Processing: System Demonstrations*, pp. 38–45, Online, October 2020. Association for Computational Linguistics. doi: 10.18653/v1/2020.emnlp-demos.6. URL <https://aclanthology.org/2020.emnlp-demos.6>.

xAI. Grok 4.1 model card, November 2025. URL <https://data.x.ai/2025-11-17-grok-4-1-model-card.pdf>.

Xia, Y., Jin, P., Xie, S., He, L., Cao, C., Luo, R., Liu, G., Wang, Y., Liu, Z., Chen, Y.-J., Guo, Z., Bai, Y., Deng, P., Min, Y., Lu, Z., Hao, H., Yang, H., Li, J., Liu, C., Zhang, J., Zhu, J., Bi, R., Wu, K., Zhang, W., Gao, K., Pei, Q., Wang, Q., Liu, X., Li, Y., Zhu, H., Lu, Y., Ma, M., Wang, Z., Xie, T., Maziarz, K., Segler, M., Yang, Z., Chen, Z., Shi, Y., Zheng, S., Wu, L., Hu, C., Dai, P., Liu, T.-Y., Liu, H., and Qin, T. Nature language model: Deciphering the language of nature for scientific discovery, 2025. URL <https://arxiv.org/abs/2502.07527>.

Xie, S., Yan, R., Guo, J., Xia, Y., Wu, L., and Qin, T. Retrosynthesis prediction with local template retrieval, 2023. URL <https://arxiv.org/abs/2306.04123>.

Xu, R., Zhang, Y., Wang, Q., Edwards, C., and Ji, H. omebench: Towards robust benchmarking of llms in organic mechanism elucidation and reasoning, 2025. URL <https://arxiv.org/abs/2510.07731>.

Xuan-Vu, N., Armstrong, D., Wehrbach, M., Bran, A. M., Jončev, Z., and Schwaller, P. Synthelite: Chemist-aligned and feasibility-aware synthesis planning with llms, 2025. URL <https://arxiv.org/abs/2512.16424>.

Yang, Y., Shi, R., Li, Z., Jiang, S., Lu, B.-L., Zhao, Q., Yang, Y., and Zhao, H. BatGPT-Chem: A foundation large model for chemical engineering. *Research*, 8:0827, 2025. doi: 10.34133/research.0827. URL <https://spj.science.org/doi/abs/10.34133/research.0827>.

Zhang, C., Lin, Q., Zhu, B., Yang, H., Lian, X., Deng, H., Zheng, J., and Liao, K. SynAsk: unleashing the power of large language models in organic synthesis. *Chem. Sci.*, 16:43–56, 2025a. doi: 10.1039/D4SC04757E. URL <https://dx.doi.org/10.1039/D4SC04757E>.

Zhang, D., Liu, W., Tan, Q., Chen, J., Yan, H., Yan, Y., Li, J., Huang, W., Yue, X., Ouyang, W., Zhou, D., Zhang, S., Su, M., Zhong, H.-S., and Li, Y. ChemLLM: A chemical large language model, 2024. URL <https://arxiv.org/abs/2402.06852>.

Zhang, S., Li, H., Chen, L., Zhao, Z., Lin, X., Zhu, Z., Chen, B., Chen, X., and Yu, K. Reasoning-driven retrosynthesis prediction with large language models via reinforcement learning, 2025b. URL <https://arxiv.org/abs/2507.17448>.

Zhang, Y., Han, Y., Chen, S., Yu, R., Zhao, X., Liu, X., Zeng, K., Yu, M., Tian, J., Zhu, F., Yang, X., Jin, Y., and Xu, Y. Large language models

to accelerate organic chemistry synthesis. *Nature Machine Intelligence*, July 2025c. doi: 10.1038/s42256-025-01066-y. URL <https://www.nature.com/articles/s42256-025-01066-y>.

Zhao, Z., Huang, Z., Li, J., Lin, S., Zhou, J., Cao, F., Zhou, K., Ge, R., Long, T., Zhu, Y., Liu, Y., Zheng, J., Wei, J., Zhu, R., Zou, P., Li, W., Cheng, Z., Ding, T., Wang, Y., Yan, Y., Wei, T., Ming, H., Mao, W., Sun, C., Liu, Y., Wang, Z., Zhang, Z., Yang, T., Ma, H., Gao, Z., and Pei, J. Superchem: A multimodal reasoning benchmark in chemistry, 2025a. URL <https://arxiv.org/abs/2512.01274>.

Zhao, Z., Ma, D., Chen, L., Sun, L., Li, Z., Xia, Y., Chen, B., Xu, H., Zhu, Z., Zhu, S., Fan, S., Shen, G., Yu, K., and Chen, X. Developing ChemDFM as a large language foundation model for chemistry. *Cell Rep. Phys. Sci.*, 6(4):102523, April 2025b. doi: 10.1016/j.xcrp.2025.102523. URL <https://doi.org/10.1016/j.xcrp.2025.102523>.

Zhong, Z., Song, J., Feng, Z., Liu, T., Jia, L., Yao, S., Hou, T., and Song, M. Recent advances in deep learning for retrosynthesis. *WIREs Computational Molecular Science*, 14(1):e1694, 2024. doi: <https://doi.org/10.1002/wcms.1694>. URL <https://wires.onlinelibrary.wiley.com/doi/abs/10.1002/wcms.1694>.

A. Models' Performance

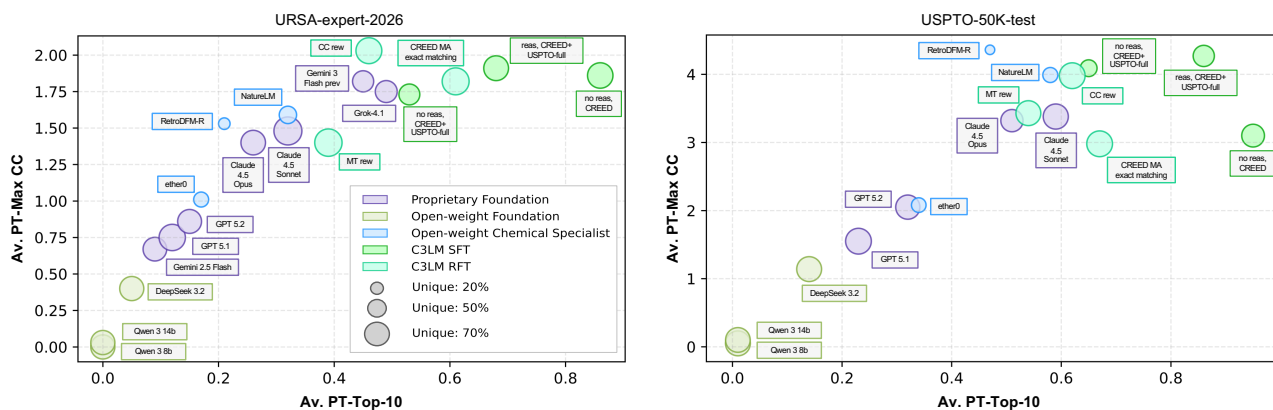


Figure 6. LLMs' performance in URSA benchmark on URSA-expert-2026 (left) and USPTO-50K-test (right) sets. Higher values along both axes indicate better performance (top-right is best).

B. Glossary

Target molecule The target molecule is the desired chemical compound that represents the ultimate goal of synthesis planning. It is the molecule for which the system generates or evaluates synthetic routes, and it serves as the starting point for retrosynthetic disconnection, working backward from the target to identify precursor molecules.

Reactants Reactants are the chemical compounds that undergo transformation during a chemical reaction and whose atoms are directly incorporated into the product structure. Technically, reactants are distinguished from reagents by the presence of atom mapping – atoms in reactants have corresponding mapped atoms in the product(s).

Reagents Reagents are chemical compounds that participate in a chemical reaction but whose atoms are not directly incorporated into the product structure. Reagents typically facilitate or enable the transformation (e.g., catalysts, bases, acids, solvents with reactive roles) with no or only minor atom contribution to the final product. For benchmarking, it is reasonable to extend the reacting species with reagents, since they may influence the correctness of atom–atom mapping and thereby the reaction-center extraction process.

Starting materials Starting materials are the initial chemical compounds from which a synthetic route begins. They are molecules that exist at the terminal nodes (leaves) of a retrosynthetic tree and are not produced by any reaction step within the route. Starting materials serve as the input chemicals for the synthesis and are expected to be commercially available or otherwise accessible within the reported synthetic methods.

Building blocks Building blocks (CABBS) are commercially available chemical compounds that can be found in vendor datasets and purchased from them.

Single-step retrosynthesis model An SSRS model predicts one or several retrosynthetic disconnections by mapping a target product molecule to a set of precursor reactants corresponding to a single reaction step. The model does not perform recursive planning or multi-step route construction, focusing instead on identifying chemically plausible reactants.

Multi-step retrosynthesis model An MSRS model is a system that applies retrosynthetic transformations (typically recursively) to decompose a target molecule into commercially available or otherwise accessible starting materials through a sequence of reaction steps.

Reaction center (RC) An RC is the set of atoms (dynamic atoms) in one or more reactant molecules and the product molecule that undergoes change during a chemical transformation, including atoms/bonds that are formed, broken, created, destroyed, or whose connectivity, bond order, formal charge, or hybridization state differs between reactants and products.

Chemical plausibility Chemical plausibility reflects alignment of a reaction with core principles of organic synthesis (e.g., chemoselectivity, regioselectivity, stereoselectivity). Operationally, it can be reduced to chemoinformatic concepts such as reaction centers, functional groups, their occurrence, and compatibility rules, potentially augmented with conditions (solvents, temperature, catalysts, auxiliary reagents). In this system, plausibility is assessed by comparing the reaction center and functional-group context against a reference dataset of verified transformations. If the extracted reaction center is absent from the reference library, the reaction is considered implausible; similarly, functional groups never observed for that reaction center negate plausibility. When both reaction-center and functional-group context are supported by precedents, the reaction is considered chemically plausible.

Level of confidence The nominal degree of chemical plausibility is estimated via discrete levels of confidence (LC), depending on which reaction-center representation is matched among verified transformations. Higher LC indicates that a more specific (larger-context) reaction-center definition is supported, correlating with higher nominal plausibility and representativeness in terms of synthetic precedents. The LC value is used as the reaction score in ChemCensor.

Functional groups (FGs) FGs are structural motifs that determine chemical reactivity and properties. In the present system, functional groups are represented as SMARTS patterns ([Daylight Chemical Information Systems, 2007](#)) that can be matched to molecular structures via substructure search. Functional-group context annotated for each reaction center helps determine which patterns are tolerable for a transformation, supporting chemical plausibility.

Functional group (FG) signature An FG signature is the ensemble of FGs present in reactant/product molecules that are not affected by the transformation. For a given reaction center, the signature is constructed by aggregating synthetic precedents from the reference dataset.

ChemCensor ChemCensor Score (CC Score) is a quantitative metric evaluating the chemical plausibility of a reaction and/or a retrosynthetic route by measuring the proportion of steps that pass plausibility validation, weighted by their confidence levels.

Reference dataset A reference dataset is a collection of verified reaction transformations extracted from sources including patents (e.g., USPTO), articles, preprints, and ELNs. It may include metadata such as conditions and yield. In this system, the reference dataset is used to validate analyzed reactions via reaction-center matching and functional-group signature comparison.

Synthetic precedent A synthetic precedent is an elementary synthetic fact of a successful chemical reaction recorded in a reference dataset.

C. When Single Answer Is Not Enough: Examples

To illustrate the weakness of ground truth-based metrics, the following target molecule (example #1) from the USPTO-50K-test set was used to predict the possible reactant sets using the RetroKNN model ([Xie et al., 2023](#)) via Syntheseus interface ([Maziarz et al., 2025](#)). In the USPTO-50K-test set, there is only one reaction, the ground truth, which is provided for model performance estimation. The reaction represents bromo-Stille cross-coupling C-C bond formation ([Figure 7](#)).

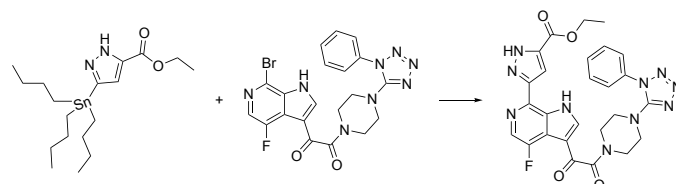


Figure 7. The ground truth for the example #1 from the USPTO-50K-test set.

Besides the reaction shown in [Figure 7](#), RetroKNN also predicts at least two other reactions since, obviously, other disconnections for the molecule are available. The first reaction proceeds as an amide synthesis, and the second one is also based on Stille cross-coupling, but for a chlorine atom. While these predictions are considered irrelevant for ground truth-based metrics, they are scored as chemically plausible by ChemCensor [Figure 8](#).

It is interesting to note that for the chloro-Stille cross-coupling, the algorithm provides the same patent application (US20070249579A1) provided for the ground truth. ChemCensor allows checking all reactions associated with the concrete

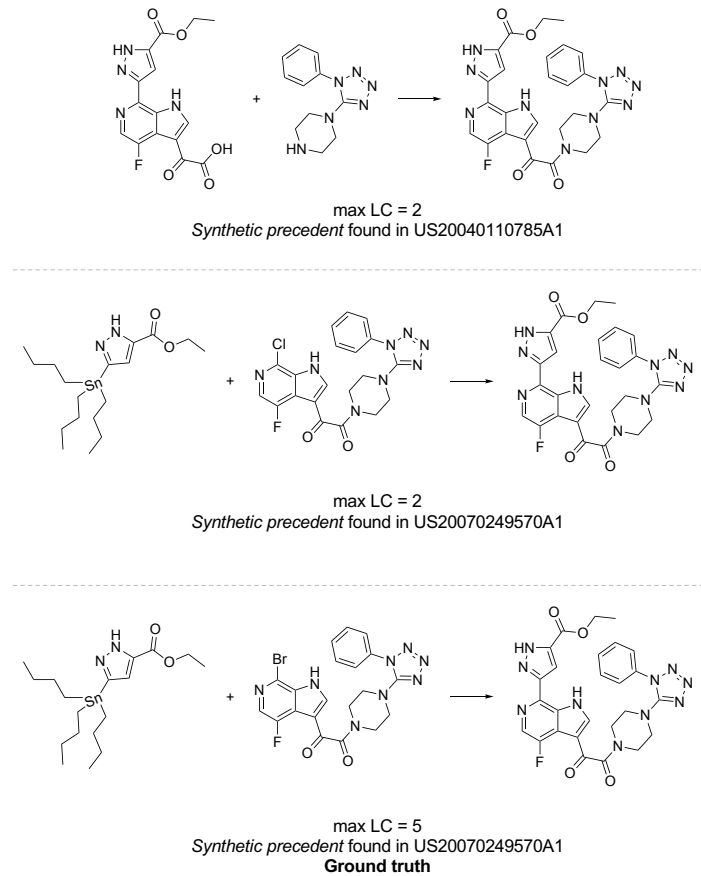


Figure 8. Scoring three different outcomes predicted by RetroKNN for example #1.

reference document ID and if one checks other reactions present in the patent with the ground-truth reaction, the chloro-Stille coupling very similar to the ground truth with a fluorine atom replaced with a methoxy group is found (Figure 9). The Top-K accuracy-based benchmark rejects this reaction, because it is not the ground truth, while it differs from the ground truth only by a methoxy group non-participating in the transformation and halogen functionality.

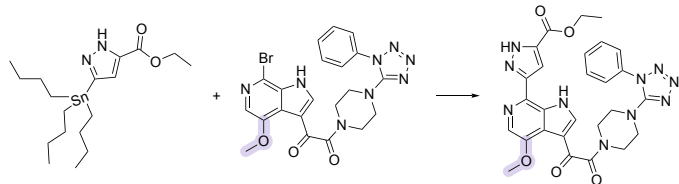


Figure 9. The additional reaction found in the patent application US20070249579A1, where the ground truth for example #1 was extracted from.

To additionally illustrate the difference between our scoring approach and commonly used metrics, another target molecule from the USPTO-50K-test, example #2, was used to predict single-step retrosynthetic output within the LocalRetro model (Chen & Jung, 2021). The target molecule and its ground truth are shown in Figure 10.

In addition to the reaction shown in Figure 10, LocalRetro also outputs at least two other transformations. The first reaction was obtained by the formation of a C-N amide bond between the core scaffold and the side chain. The second one represents iodo-Suzuki cross-coupling. Although these predictions are considered chemically plausible by ChemCensor, they are deemed irrelevant for the ground truth-based metrics (Figure 11). Interestingly, for the second transformation, the ChemCensor Score is 1, highlighting the degree of exclusiveness for iodo-pyrazolopyridine substrate in the Suzuki reaction.

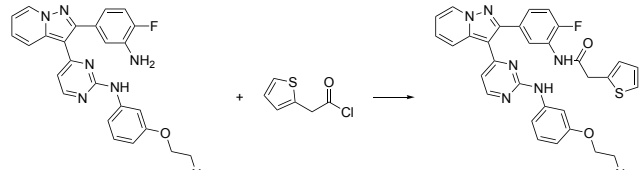
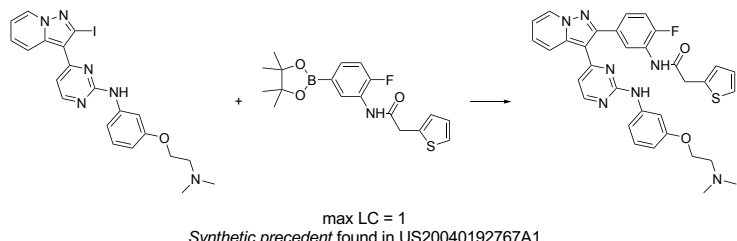
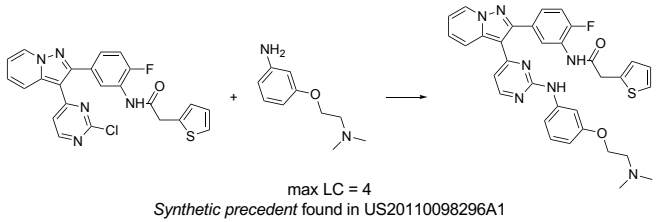
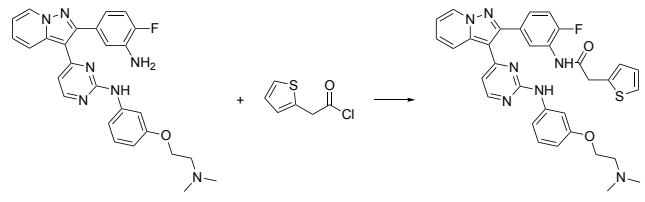


Figure 10. The ground truth for example #2.



max LC = 1
Synthetic precedent found in US20040192767A1



max LC = 5
Synthetic precedent found in US20090149456A1
Ground truth

Figure 11. Scoring three different outcomes predicted by LocalRetro for example #2.

The examples provided illustrate the advantages of the present ChemCensor as a tool to assess SSRS models' output. It is not biased to the ground truth concept and provides the user with a powerful engine for single reaction evaluation.

D. ChemCensor Details

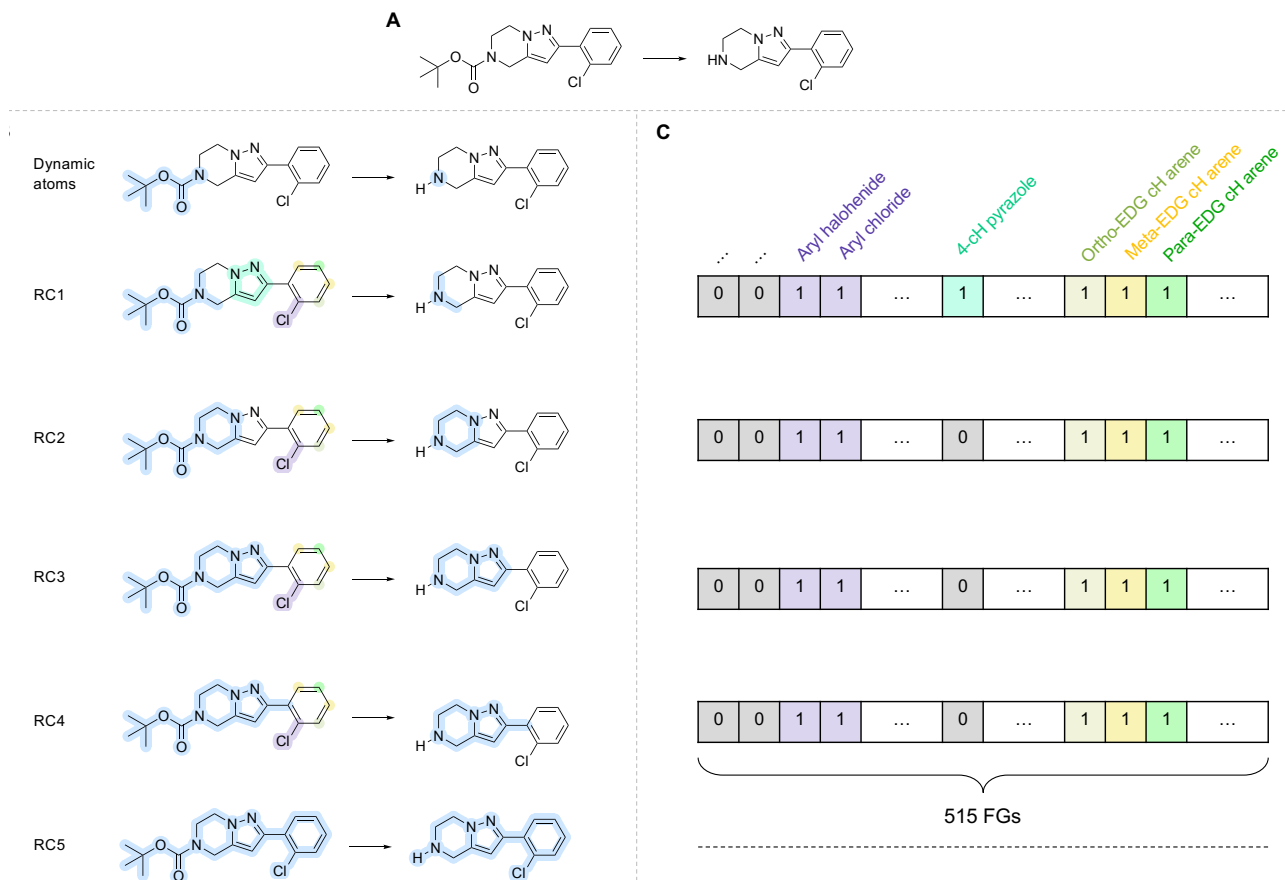


Figure 12. ChemCensor operands. **A.** Input reaction. **B.** RCNs (highlighted in blue). **C.** FG signatures (FGs are highlighted).

D.1. Reaction center (RC)

In this work, we distinguish five levels of reaction center annotation, denoted RC1, RC2, RC3, RC4 and RC5 corresponding to confidence levels and ChemCensor Scores 1, 2, 3, 4 and 5, respectively. The RCN is the representation of an RC, where N shows the size of the substructural context of an RC; the higher the N, the higher the context size (see Figure 12 B):

- RC1 represents the minimal local environment of RC, which is defined by the atoms changing their connectivity within a reaction (dynamic atoms) and atoms at topological distance of 1 around dynamic atoms. Also, RC1 includes atoms from predefined FGs (e.g., carbonyl group, nitrile, etc.) when at least one atom of a FG is dynamic. Therefore, RC1 defines the most compact representation of the RC sufficient to capture the immediate chemical transformation.
- While RC2 includes atoms from RC1, it also reflects more substructural context around an RC, incorporating the local ring context, stereochemical surroundings, and/or the atoms at topological distance of 2 around dynamic atoms
- RC3 further extends the substructural context of RC2 by adding fused-ring connectivity context around a RC and/or the atoms at topological distance of 3 around dynamic atoms.
- Finally, RC4 provides the most extended description of an RC, adding substituent context to aromatic systems: one atom of the rings' substituents with extension of predefined FGs (e.g., carbonyl group, nitrile, etc.) and/or the atoms at topological distance of 4 around dynamic atoms.

Technically, RCN is the set of canonicalized SMARTS-like objects describing reacting patterns for both left and right sides of the reaction. To expedite the searching, they are handled simply as strings and stored as a library of reaction centers together with their annotated FG signatures.

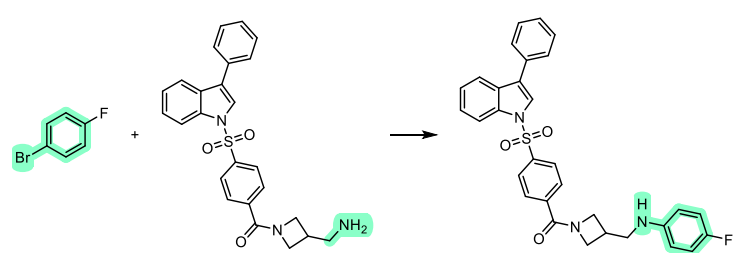
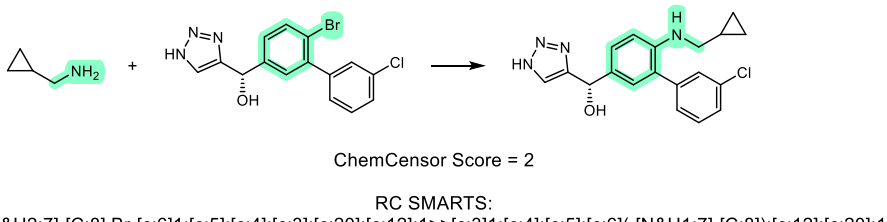
D.2. Functional group (FG)

Each RC is equipped with non-reacting FGs compatible with it, based on established *synthetic precedents*. To verify that the non-reacting FGs identified in the reaction to be scored are compatible with the RC algorithm generates a FG signature that can be compared with the reference dataset.

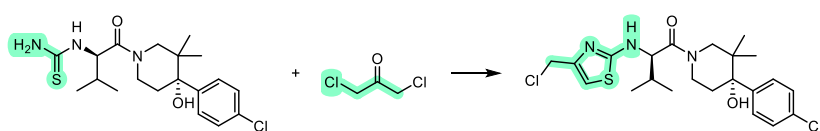
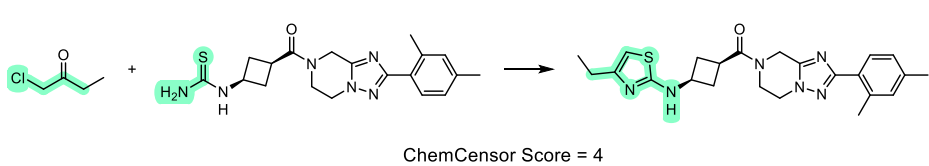
The ChemCensor algorithm uses a curated database of 515 functional group patterns that covers basic chemical entities relevant to organic chemistry. For computational simplicity, it is encoded as a 515-bit signature, annotated for each RC based on functional groups found in the static (non-reaction-center) parts of the molecular structure. A non-reacting FG is considered present if all the atoms of FG are not overlapped with RC atoms (Figure 12 C). Thus, for different RCN in a single reaction, the FG signatures may differ. During the annotation of centers in the reference dataset, a FG signature is created that accounts for all reaction examples (*synthetic precedents*) associated with the given RC.

E. Reaction Examples and Detailed ChemCensor Output

This section illustrates ChemCensor scoring and annotation for example reactions sampled from predictions of the C3LM SFT model with reasoning for URSA-expert-2026. We picked 5 examples to highlight different pass and non-pass categories. In Figure 13, two reactions which fully passed ChemCensor in terms of both the RC and FG combination precedence are outlined. For each valid reaction, the module provides extracted mapped SMARTS of the reaction center, reference document ID and the respective synthetic precedent example.



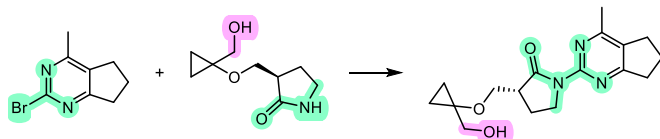
Synthetic precedent with the same RC. The document ID: US20070088018A1



Synthetic precedent with the same RC. The document ID: US20070208056A1

Figure 13. Example reactions predicted by the C3LM SFT model which passed ChemCensor.

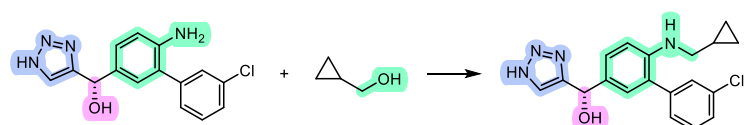
If the input reaction is not reflected by the reference dataset of synthetic precedents in terms of its RC and FG context, ChemCensor provides a zero score and the reaction can be considered as chemically implausible. In that case, the module prints the exact reason of failure: (1) there are no precedents of RC representations or (2) the presence of specific non-participating functional groups is not reported for the found RC precedent. In the latter situation, ChemCensor returns the full list of functional groups that violate chemo-/regioselectivity knowledge extracted from the reference dataset (Figure 14).



ChemCensor Score = 0

 RC SMARTS:
Br-[c:4](:[n:3]):[n:18].[N&H1:5](-[C:6])- [C:16]=[O:17]>>[n:3]:[c:4](-[N:5](-[C:6])- [C:16]=[O:17]):[n:18]

No synthetic precedents with the following FGs: Primary alcohol



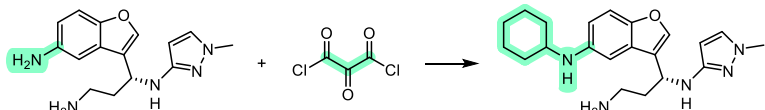
ChemCensor Score = 0

 RC SMARTS:
[c:3]1:[c:4]:[c:5]:[c:6](-[N&H2:7]):[c:12]:[c:20]1.O-[C&H2:8]-[C:9]>>[c:3]1:[c:4]:[c:5]:[c:6](-[N&H1:7]-[C&H2:8]-[C:9]):[c:12]:[c:20]1

No synthetic precedents with the following FGs: Secondary alcohol, Azole

Figure 14. Example reactions which didn't pass ChemCensor due to functional group incompatibility.

Reactions for which reaction center representations are absent from the reference dataset are annotated with extracted mapped SMARTS only and a message of absence of synthetic precedents (Figure 15).



ChemCensor Score = 0

 RC SMARTS:
[c:17]-[N&H2:18].O=[C:19](-Cl)-[C:23](=O)-[C:22](=O)-Cl>>[c:17]-[N&H1:18]-[C&H1:19]1-[C&H2:20]-[C&H2:21]-[C&H2:22]-[C&H2:23]-[C&H2:24]-1

No synthetic precedents with this RC

Figure 15. A reaction example for which RC representations are absent from the reference dataset.

F. Functional Groups With The Highest FG-related Error Rate

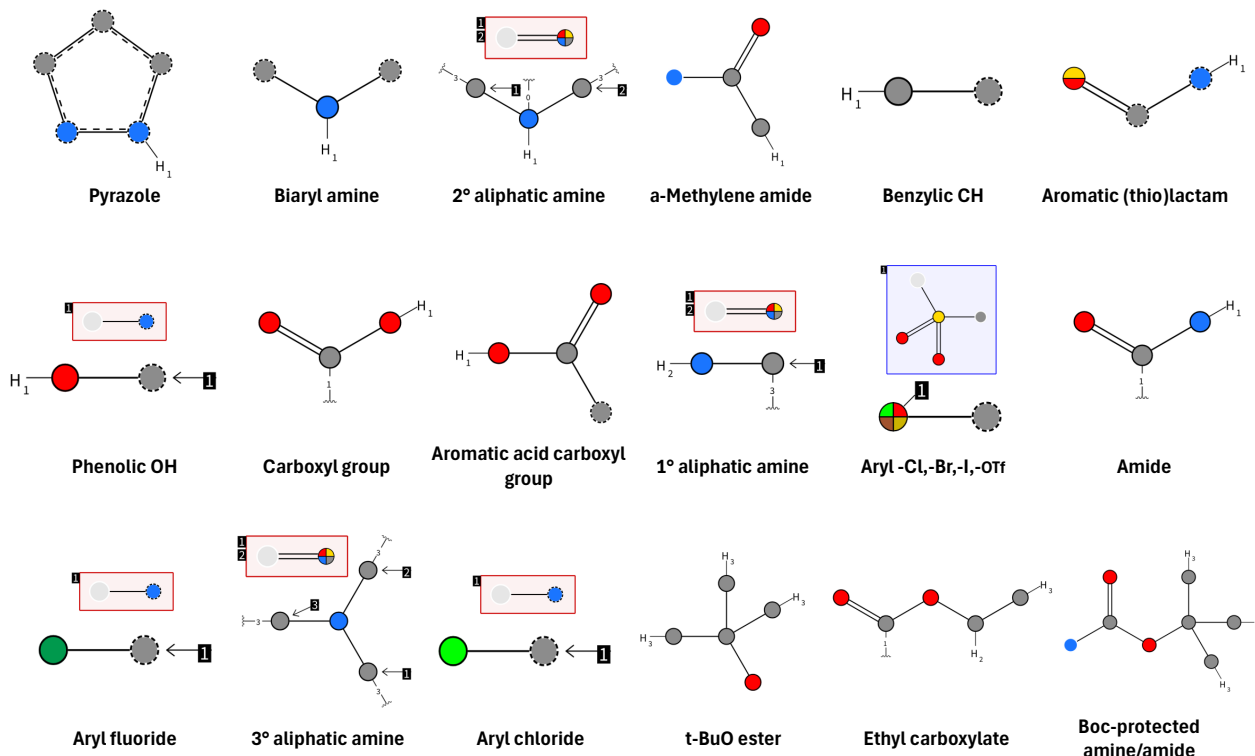


Figure 16. Visualized SMARTS patterns for FGs with the highest FG incompatibility error count across the Top-10 models by means of **Av. PT-Top-10 CC**. Individual figure preparation was performed in (Ehrt et al., 2020).

G. CREED Details

CREED splitting The splitting was performed randomly while preserving the distribution of the number of reactions per product, ensuring that identical products appear in *only one* split. The splitting summary is provided in Table 3.

Intersection with publicly available reaction dataset (USPTO-full): 7,147 (0.12% of all reactions in CREED).

Product molecules in the CREED were ensured to be free of targets in both holdout sets: the URSA-expert-2026 and the USPTO-50K-test sets. Moreover, Tanimoto similarities (Morgan fingerprints, radius=2, 2048 bits) between CREED's product molecules and molecules from both sets were calculated to identify similar entities. For the URSA-expert-2026, the most similar molecule had a Tanimoto coefficient of 0.523, highlighting the utility of this holdout set for assessing the generalization power of models trained on URSA-expert-2026. For the USPTO-50K-test set, 30 molecules showed similarity higher than 0.85, with 14 molecules showing similarity equal to 1.0 and different only in stereochemistry.

Figure 18 illustrates the chemical capacity of CREED. While USPTO-full typically provides only a limited number of transformations, CREED yields a substantially larger and more diverse set of associated reaction examples (verified by ChemCensor), enabling a richer characterization of plausible disconnections and reducing benchmark sparsity for a given product.

Figure 19 illustrates some reaction examples from CREED for the product molecule, which is not included in USPTO-full.

Statistic	Value
Global	
Unique reactions	6,382,667
Unique products	653,567
Reactions per product	
Min	1
Max	72
Mean	9.77
Median	8.00
Std	7.78
Reactions statistics by number of components	
1-component	3,834,173 (60.07%)
2-component	2,547,502 (39.91%)
3-component	908 (0.01%)
4-component	84 (< 0.01%)

Table 2. Summary statistics of CREED.

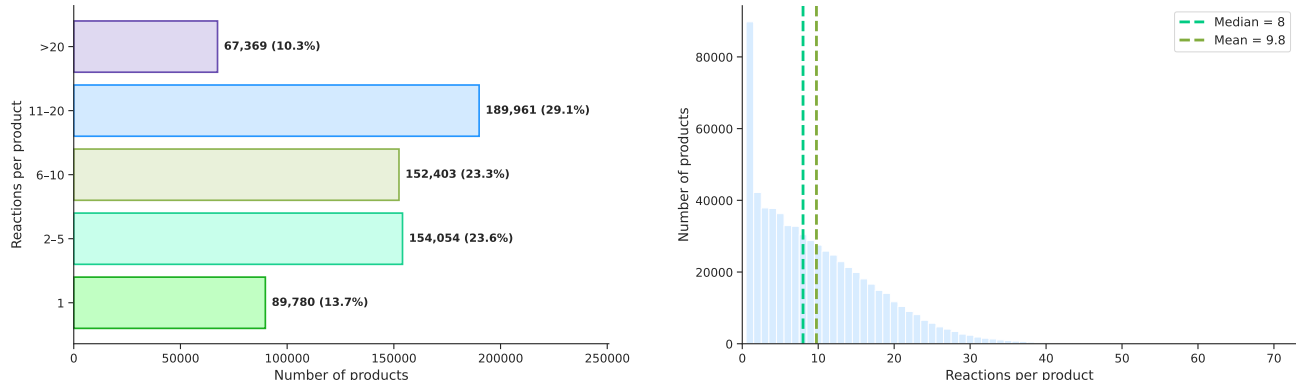


Figure 17. CREED dataset distributions of reactions per product: (left) distribution by category; (right) overall distribution.

Split	Unique reactions	Unique products
Train	5,107,681	522,865
Validation	635,977	65,285
Test	638,184	65,350

Table 3. CREED split-level statistics.

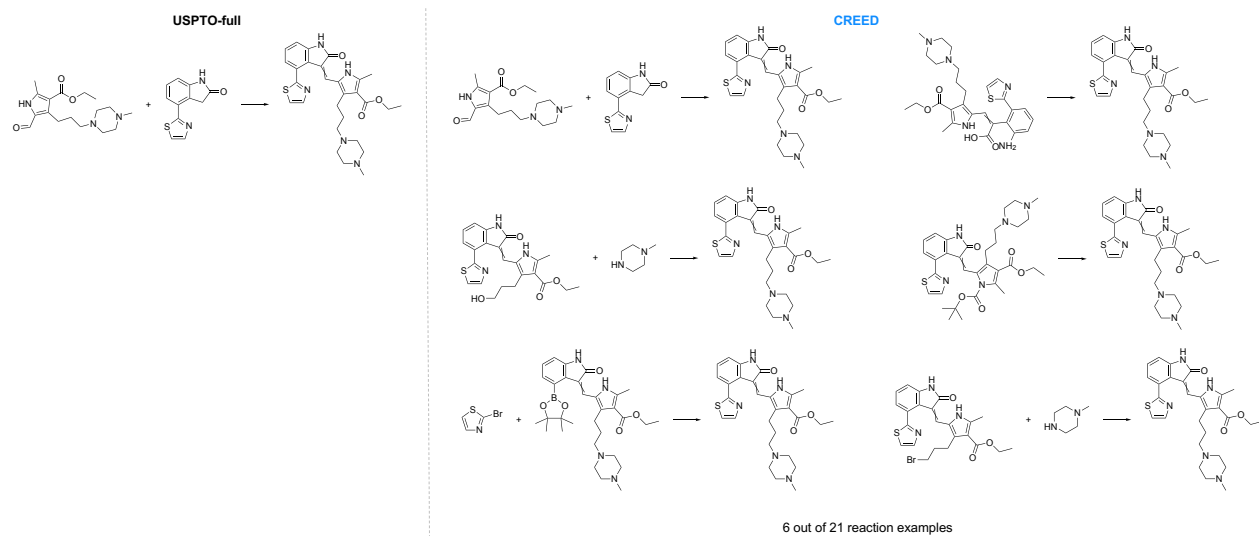


Figure 18. Reaction examples for particular product molecule from USPTO-full (left) and CREED (right).

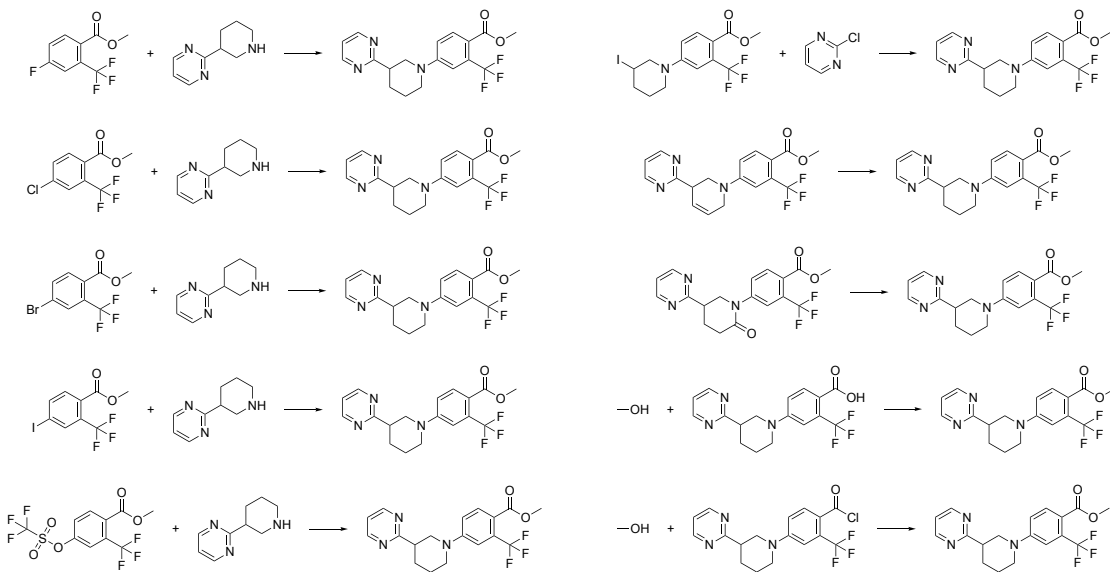


Figure 19. Examples of reactions from CREED for the product molecule, which is not included in USPTO-full.

H. C3LM Model Training Details

C3LM is supervised fine-tuned on CREED using the AdamW optimizer with a learning rate of 1×10^{-5} , a linear warmup over the first 2,000 steps, and a cosine learning-rate schedule thereafter.

C3LM RFT models were trained using GRPO with one of three verifiable reward functions. Each of the three RFT models share all training hyperparameters. The prompts for the GRPO groups were sampled from the same CREED training set as SFT in groups of 16 with completions were generated with a temperature of 1.2. The number of updates per batch (number of iterations, μ) was set to 1 and the KL penalty (β) set to 0.05. The groups of 16 completions were sampled in batches of 8 unique prompts for a global batch size of 128. Each model was trained on a single node with 8 NVIDIA B200 GPUs. Deepspeed stage 3 (Rasley et al., 2020) was used, with gradient checkpointing and BF16 precision. The AdamW optimizer was used for each model with learning rate 1×10^{-6} at constant schedule and no learning rate warmup, as well as weight decay of 0.05. The token throughput was approximately 20,000 tokens per global step and each model was trained for approximately 5000 steps or stopped early if suitable reward convergence or significant model deviation was observed.

I. Templates Used for Benchmarking and C3LM training

To formulate retrosynthesis tasks in natural language, we use a set of modified templates from MolInstructions (Fang et al., 2024). We wrap each pair of product and reactants into fifteen different templates, forming the final data representation. These templates in Jinja2 format are listed below.

Templates for the retrosynthesis task

Template 1

Based on the given product, provide some plausible reactants that might have been utilized to prepare it:
<smiles>{{source}}</smiles>.

Template 2

Can you identify some reactants that might result in the given product: <smiles>{{source}}</smiles>?

Template 3

Given the following product <smiles>{{source}}</smiles>, please provide possible reactants.

Template 4

Given the product provided <smiles>{{source}}</smiles>, propose some possible reactants that could have been employed in its formation.

Template 5

Given these product <smiles>{{source}}</smiles>, can you propose the corresponding reactants?

Template 6

Please suggest possible reactants for the given product: <smiles>{{source}}</smiles>

Template 7

Please suggest potential reactants for the given product: <smiles>{{source}}</smiles>

Template 8

Please suggest potential reactants used in the synthesis of the provided product: <smiles>{{source}}</smiles>

Template 9

Provide a list of potential reactants that may have produced the given product: <smiles>{{source}}</smiles>

Template 10

Provided the product below, propose some possible reactants that could have been used in the reaction: <smiles>{{source}}</smiles>

Template 11

What are the possible reactants that could have formed the following product <smiles>{{source}}</smiles>?

Template 12

What reactants could lead to the production of the following product <smiles>{{source}}</smiles>?

Template 13

Which reactants could have been used to generate the given product <smiles>{{source}}</smiles>?

Template 14

With the given product <smiles>{{source}}</smiles>, suggest some likely reactants that were used in its synthesis.

Template 15

With the provided product <smiles>{{source}}</smiles>, recommend some probable reactants that were likely used in its production.

J. USPTO-50K-test Set

The original **USPTO-50K** splits for train, validation and test subsets were introduced in (Liu et al., 2017) and can be accessed on the GitHub repository:

- Sources (SMILES strings of products): https://github.com/pandegroup/reaction_prediction_seq2seq/blob/master/processed_data/test_sources
- Targets (SMILES strings of reactants): https://github.com/pandegroup/reaction_prediction_seq2seq/blob/master/processed_data/test_targets

The original test set contains 5004 reactant–product pairs. We removed 28 entries that were clearly corrupted or ill-posed for retrosynthesis evaluation (see Table 4).

These exclusions target unambiguous dataset artifacts that undermine the benchmark semantics. In particular, we found cases where molecules (e.g., trifluoroacetic acid or maleic/fumaric acid) appear as the *product*, which is most consistent with preprocessing or role-assignment errors (e.g., reagent/solvent leakage into the product field) rather than meaningful synthetic targets. We also removed entries with obvious processing artifacts and targets with molecular weight below 100 Da. Overall, this conservative curation reduces evaluation noise and makes reported metrics more representative of performance on chemically meaningful targets.

The modified **USPTO-50K-test** was used as a holdout set. The **CREED** and **USPTO-full** were strictly decontaminated with **USPTO-50K-test**, so the training datasets for our models don't contain reactions (and product molecules) from holdout at all.

SMILES of product	SMILES of reactants	Reason	Removed indexes (from the original dataset, starting from 0)				Removed count
<chem>FC(F)(=O)O</chem>	<chem>CNCCc1ccncc1</chem> <chem>O=C1C=CC2=C1C(O)=C3C(=O)N2Cc4ccccc4Cl</chem>	Trifluoro acetic acid (TFA) as a product. Artifact of reaction processing.	144	350	3281	4086	
			161	1644	3321	4482	20
			200	1666	3753	4605	
			204	2664	3990	4985	
			295	3260	1647	4992	
<chem>Oc1ccccc1</chem>	<chem>CC(C)(C)OC(=O)N1CCN(Cc2ccc(F)cc2)CC(O)c3ccccc3</chem>	Maleic or fumaric acid as a product. Artifact of reaction processing.	727	2250	2566	4380	4
--		Other artifacts of reaction processing.	433	2390	3084	4453	5
--		MW of product < 100 Da.	497				
			645	1526	3929		3
							In total 32

Table 4. Items removed from the USPTO-50K test set.

K. URSA-expert-2026 Set

The SMILES strings of molecular structures from the URSA-expert-2026 set are provided in [Table 5](#). The 2D structures are provided in [Table 6](#).

The dataset diversity is 0.85886. Dataset diversity is defined as the average pairwise dissimilarity between all distinct molecule pairs:

$$\text{Diversity} = \frac{1}{N(N-1)} \sum_{i \neq j} (1 - \text{Similarity}(i, j)), \quad (5)$$

where N is the number of molecules in the dataset.

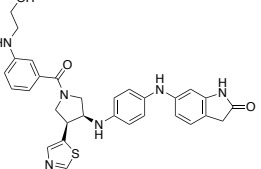
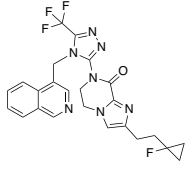
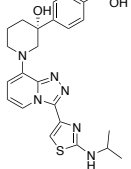
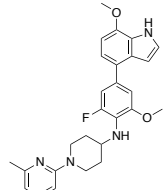
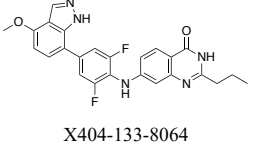
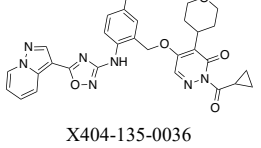
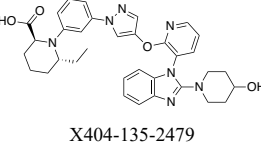
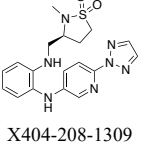
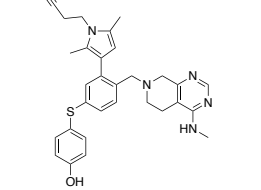
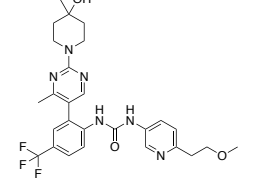
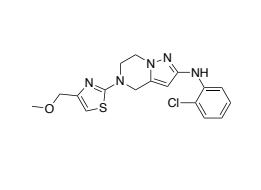
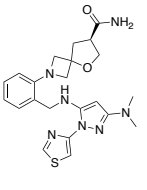
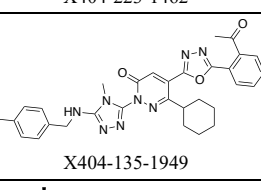
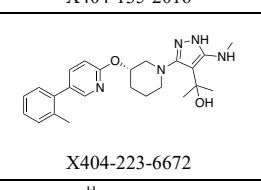
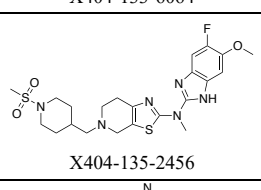
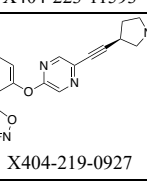
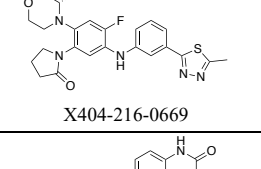
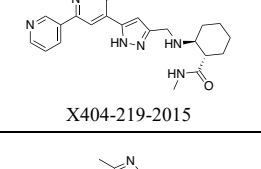
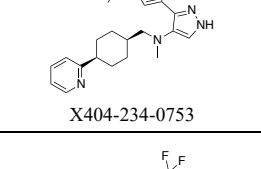
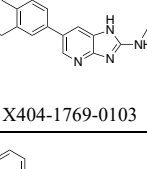
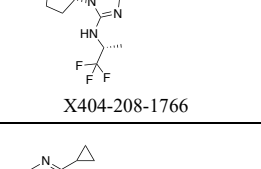
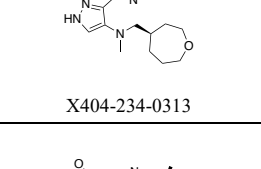
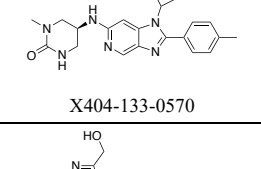
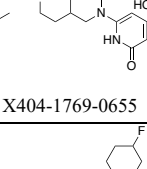
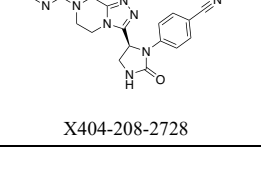
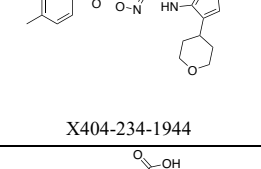
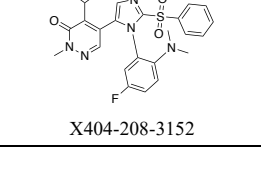
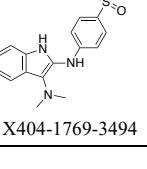
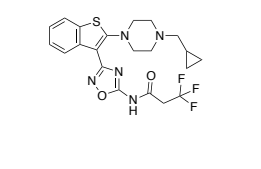
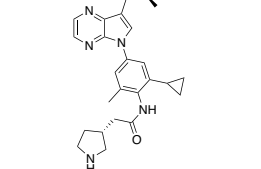
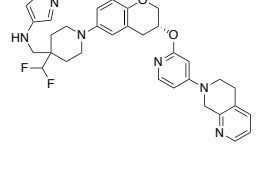
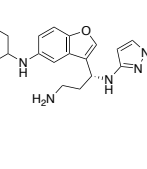
Molecular similarity in [Equation 5](#) is computed as the cosine similarity between binary vectors of structural screens, where each vector element indicates the presence or absence of a specific atom-centered structural fragment derived using the Chemosoft software (ChemDiv Inc. chemical database software, <https://www.chemdiv.com/>). The set of screens is constructed dynamically across the dataset, capturing atom types, bond types, and ring environments without using hash-based compression.

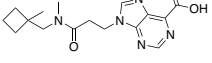
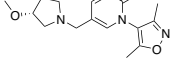
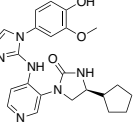
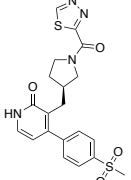
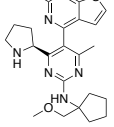
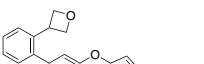
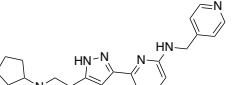
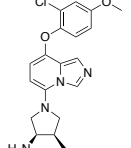
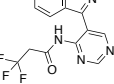
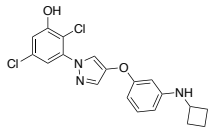
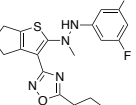
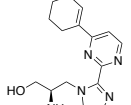
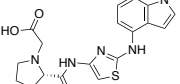
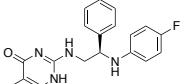
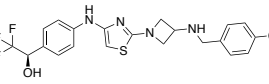
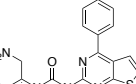
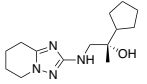
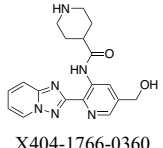
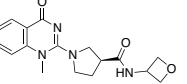
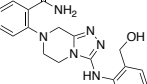
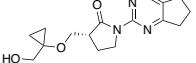
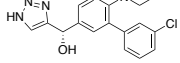
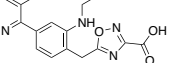
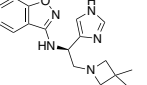
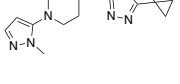
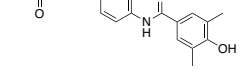
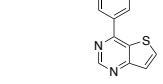
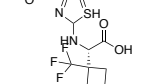
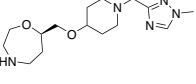
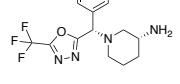
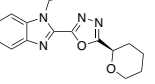
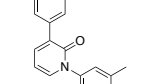
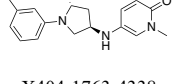
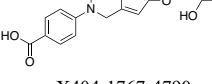
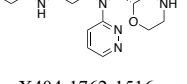
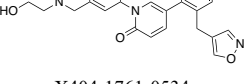
Table 5. URSA-expert-2026 set.

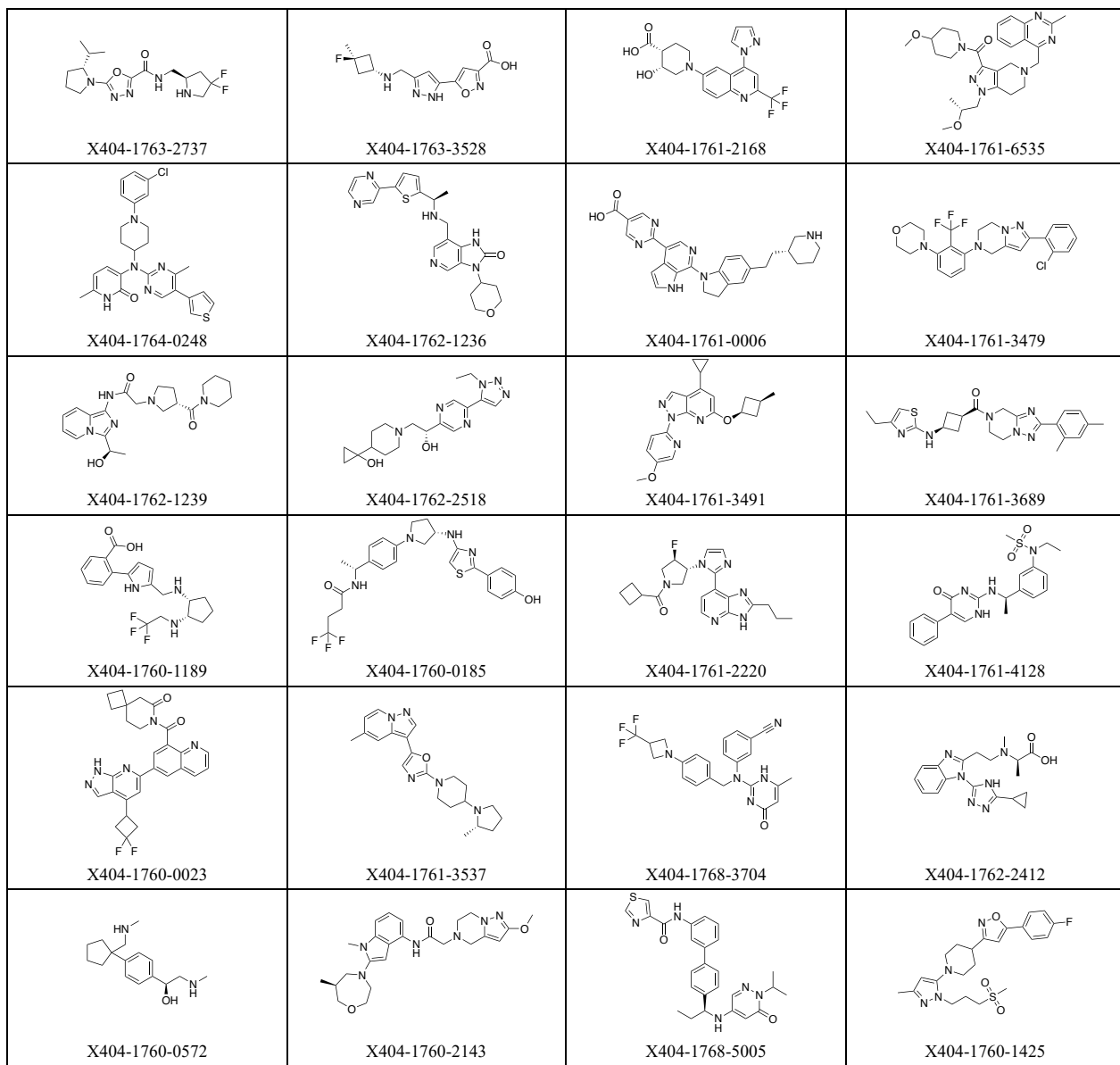
ID	SMILES
X404-223-1421	O=C1Cc2ccc (Nc3ccc (N[C@H]4CN (C(=O)c5cccc (NCCO)c5) C[C@H]4c4cnccs4) cc3) cc2N1
X404-133-8064	CCC1nc2cc (Nc3c(F)cc (-c4ccc (OC)c5cn [nH]c45) cc3F) ccc2c(=O) [nH]1
X404-223-1462	CNc1ncnc2c1CCN (Cc1ccc (Sc3ccc (O)cc3) cc1-c1cc (C)n (CCC#N)c1C) C2
X404-135-1949	CC(=O)c1cccc1-c1nncc (-c2cc(=O)n (-c3nncc (Nc4ccc (Cl)cc4) n3C) nc2C2CCCCC2) o1
X404-219-2456	O=C1c2nc (CCC3(F)CC3) cn2CCN1c1nncc (C(F)(F)F) n1Cc1cncc2cccc12
X404-135-0036	Cc1ccc (Nc2noc (=O)c3ccn4cccc34) n2) c (Coc2cnn (C(=O)C3CC3) c(=O)c2C2CCOCC2) c1
X404-135-2016	COCCc1cc (NC(=O)Nc2ccc (C(F)(F)F)cc2-c2cnc (N3CCC(C)(O)CC3) nc2C) cn1
X404-223-6672	CNc1c[nH]nc (N2CCC[C@H] (Oc3ccc (-c4cccc4C) cn2) c1C (C) (C) O
X404-223-10866	CC(C)Nc1nc (-c2nncc3c (N4CCC[C@H](O)c5ccc (CO)cc5)C4) cccn23) cs1
X404-133-6064	COCC1csc (N2CCn3nc (Nc4cccc4C1) cc3C2) n1
X404-135-2456	Co1cc2[nH]c (N(C)c3nc4(s3)CN (CC3CCN (S(C)(=O)=O)C3)CC4)nc2cc1F
X404-135-2479	CC[C@H]1CCCC[C@H](C(=O)O)N1c1cccc (-n2cc (Oc3cccc3-n3C(N4CCC(O)CC4)nc4cccc43) cn2) c1
X404-216-0669	Cc1nncc (-c2cccc (Nc3cc (N4CCCC4=O)c (N4CCO[C@H](C)[C@H]4C#N)cc3F) c2) s1
X404-208-1766	C[C@H](Nc1nc (-c2ccc3[nH]c(=O)cnc3c2) nn1[C@H]1CCN1) C(F)(F)F
X404-133-0167	COc1cc (-c2ccc (OC)c3[nH]ccc23) cc(F)c1NC1CCN (c2cncc (C)n2)CC1
X404-223-11593	CN(C)c1cc (Nc2cccc2N2CC3 (C[C@H](C(N)=O)CO3)C2) n (-c2cscn2) n1
X404-219-0927	C(#[C]#[C@H]1CCN1) c1nc (Oc2cccn2-c2ncn2) cn1
X404-208-1309	CN1[C@H](Cncc2cccc2N2cc (-n3nncc3) nc2)CCS1(=O)=O
X404-208-2728	N#Cc1ccc (N2C(=O)NC[C@H]2c2nncc3n2CCN (c2nnccn2C2CC2)C3)cc1
X404-234-0753	Co1ccc (-n2[nH]cc2N(C)C[C@H]2CC[C@H](c3ccccc3)CC2) on1
X404-133-0570	Cc1ccc (-c2nc3nc (N[C@H]4CNC(=O)N(C)C4)cc3n2C2CC(F)(F)C2)cc1
X404-208-3152	CN(C)c1ccc (F)cc1-n1c (-c2cnn (C)c(=O)c2-c2cc (CO)n[nH]2)cnc1S(=O)(=O)c1cccc1
X404-219-2015	CNC(=O)[C@H]1CCCC[C@H]1NCC1cc (-c2cc (-c3ccncc3) n[nH]c2=O) [nH]n1
X404-234-0313	C1cnoncl -c1[nH]cc1N(C)C[C@H]1CCCCOCC1
X404-234-1944	Cc1ccc (S(=O)(=O)Cc2nc ([C@H](C)Nc3nn(C)cc3C3CCOCC3) no2)cc1
X404-1769-0103	Cc1ccc (-c2cnc3nc (Nc4cccon4) [nH]c3c2) cc1CC1CCNCC1

ID	SMILES
X404-1769-0655	CCo1cccc1-c1cccc (N2CCC (CN (C) c3cc (C4 (O) COC4) cc (=O) [nH] 3) CC2) c1
X404-1769-3494	CN (C) c1c (Nc2ccc (S (=O) (=O) N3CCC (F) CC3) cc2) [nH] c2cccc12
X404-1769-3011	O=C (CC (F) (F) F) Nc1nc (-c2c (N3CCN (CC4CC4) CC3) sc3cccc23) nol
X404-1769-1627	Cc1cc (-n2cc (C [C@H] (C) C (=O) O) c3nccn32) cc (C2CC2) c1NC (=O) C [C@H] 1CCNC1
X404-1769-3571	CN (CC1 (C) CCC1) C (=O) CCn1cnc2c (C (=O) O) ncnc21
X404-1769-4280	CO [C@H] 1CN (Cc2ccc (-O) n (-c3c (C) noc3C) c2) C [C@H] 1F
X404-1768-0001	FC (F) C1 (CNc2cnoc2) CN (c2ccc3c (c2) C [C@H] (O) c2cc (N4CCc5cccc5C4) ccn2) CO3) CC1
X404-1768-6593	Cn1ccc (N [C@H] (CCN) c2coc3ccc (NC4CCCC4) cc23) n1
X404-1768-0722	Cc1cc (-n2ccnc2Nc2ccnc2N2C [C@H] (C3CCCC) NC2=O) ccc10
X404-1768-1481	CS (=O) (=O) c1ccc (-c2cc [nH] c (=O) O) c2C [C@H] 2CCN (C (=O) c3nncs3) C2) ccl
X404-1768-3854	COCC1 (Nc2nc (C) c (-c3nc (C) nc4cccc34) c ([C@H] 3CCCN3) n2) CCCCC1
X404-1768-3154	Cn1nc (Oc2cccc (-c3cccc3C3COC3) c2) cc1CCO
X404-1768-2834	O=C (CC (F) (F) F) Nc1ncnc1-c1nn (C2CC2) c2cccc12
X404-1767-0002	Oc1cc (C1) cc (-n2cc (Oc3cccc (NC4CCC4) c3) cn2) c1C1
X404-1767-1147	O [C@H] (CNC1CCCC1) c1cc (-c2cccc (Ncc3cccc3) n2) n [nH] 1
X404-1767-0220	COc1ccc (Oc2ccc (N3C [C@H] (C) [C@H] (N) C3) n3cnnc23) c (C1) c1
X404-1767-2533	CCC (C) C1cnc (-c2c (N (C) Nc3cc (F) cc (F) c3) sc3c2CCC3) nol
X404-1767-2293	N [C@H] (CO) Cn1ccnc1-c1nccc (C2=CCCC2) n1
X404-1767-1670	O=C (O) CN1CCC [C@H] 1C (=O) Nc1sc (Nc2cccc3 [nH] ccc23) n1
X404-1769-2917	Cc1 [nH] c (NC [C@H] (Nc2ccc (F) cc2) c2ccc (F) cc2) nc (=O) c1C
X404-1766-2225	C [C@H] (O) (CNc1nc2n (n1) CCCCC2) C1CCCC1
X404-1766-0360	O=C (Nc1c (CO) cn1c1-c1n2ccccn2n1) C1CCNCC1
X404-1766-0764	Cc1nc (N2CC [C@H] (CO) C3C3 (CO) CC3) C2=O) nc2c1CCC2
X404-1766-0001	O [C@H] (c1ccc (NCC2CC2) c (-c2cccc (C1) c2) c1) c1c [nH] nn1
X404-1766-0908	COC1 (c2nnc ([C@H] (C) C3CCN (c4ccnn4C) CC3) o2) CC1
X404-1766-2761	Cc1cc (-c2nc (=O) c3cc (N4CCC [C@H] (C (=O) O) C4) ccc3 [nH] 2) cc (C) c1O
X404-1766-1829	Oc1ccc (CNC2CN (c3nc (Nc4ccc ([C@H] (O) C (F) (F) F) cc4) cs3) C2) ccl
X404-1765-6158	CC (C) [C@H] (C) (CN) NC (=O) Nc1nc (-c2ccc (O) cc2) c2ccsc2n1
X404-1765-2441	Cn1c (N2CC [C@H] (C (=O) NC3COC3) C2) nc (=O) c2cccc21
X404-1765-2945	NC (=O) c1cccc11N1CCn2c (nnc2n2cccc2CO) C1
X404-1765-3286	CCNc1cc (-c2ncc (O) c2C) ccc1Cc1nc (C (=O) O) nol
X404-1765-0440	CC1 (C) CN [C [C@H] (Nc2ncc3cccc23) c2c [nH] cn2) C1
X404-1765-0653	CCOC [C@H] 1CC (=O) N (c2cc (C1) cc (-c3ncnc4ccsc34) c2) C1
X404-1765-1623	N#Cc1cccc1c (=O) Nc1sc (N [C@H] (C (=O) O) C2 (C (F) (F) F) CCC2) n1
X404-1763-4916	Cn1nc (C (=O) N2CC (OC [C@H] 3CCNCCO3) CC2) n1
X404-1763-2878	N [C@H] 1CCCN ([C@H] (c2cccc2) c2nnc (C (F) (F) F) o2) C1
X404-1763-4338	Cc1cccc (N2C [C@H] (Nc3ccc (=O) n (C) c3) C [C@H] 2C (=O) O) c1
X404-1767-4790	Cc1ccc (O) c ([C@H] (C) 0c2cc3n (n2) CCN (c2ccc (C (=O) O) cc2) C3) c1
X404-1763-2737	Cc (C) [C@H] 1CCCN1c1nnc (C (=O) NC [C@H] 2CC (F) (F) CN2) o1
X404-1763-3528	C [C@H] 1 (F) C [C@H] (Ncc2cc (-c3cc (C (=O) O) no3) [nH] n2) C1
X404-1764-0248	Cc1ccc (N (c2ncc (-c3ccsc3) c (C) n2) C2CCN (c3cccc (C1) c3) CC2) c (=O) [nH] 1
X404-1762-2412	C [C@H] (C (=O) O) N (C) CCc1nc2cccc2n1-c1ncc (C2CC2) [nH] 1
X404-1762-1236	C [C@H] (Nc1cncc2c1 [nH] c (=O) n2C1CCOCC1) clccc (-c2ccccn2) s1
X404-1762-1239	C [C@H] (O) c1nc (NC (=O) CN2CC [C@H] (C (=O) N3CCCC3) C2) c2cccc2
X404-1762-2518	CCn1nncc1-c1nc ([C@H] (O) CN2CCC (C3 (O) CC3) CC2) cn1
X404-1762-3779	C [C@H] (CC (F) F) n1c (-c2ncc ([C@H] 3CCCCCO3) o2) nc2cccc21
X404-1762-5054	Cc1ccc (-n2cccc (-c3ccc ([C@H] (OC) (C) F) C (N) =O) c (C) c3) c2=O) c1
X404-1762-1516	Cc1ccc (Nc2cccc2F) cc1N (C [C@H] 1CNCCO1) c1ccnn1
X404-1761-0534	Cc1ccc (Cc2cnoc2) c (-c2ccc (=O) n (-c3cc4c (nn3) CCN (CCO) C4) c2) c1
X404-1761-2168	O=C (O) [C@H] 1CCN (c2ccc3nc (C (F) (F) F) cc (-n4cccn4) c3c2) C [C@H] 1O
X404-1761-6535	COC1CCN (C (=O) c2nn (C [C@H] (C) OC) c3c2CN (Cc2nc (C) nc4cccc24) CC3) CC1
X404-1761-0006	O=C (O) c1nc (-c2nc (N3Cc4cc (CC [C@H] 5CCNC5) ccc43) c3 [nH] ccc23) ncl
X404-1761-3479	FC (F) (F) c1c (N2CCOCC2) cccc1N1Cn2nc (-c3cccc3C1) cc2C1
X404-1761-3491	CCo1ccc (-n2ncc3c (C4CC4) cc (O [C@H] 4C [C@H] (C) C4) nc32) ncl
X404-1761-3689	Cc1csc (N [C@H] 2C [C@H] (C (=O) N3CCn4nc (-c5ccc (C) cc5C) nc4C3) C2) n1
X404-1764-1035	N [C@H] (C1c1ccn (Oc2cccc2-c2cccc2-c2ccc (=O) n ([C@H] 3C [C@H] (F) C3) c2) c1) C (=O) O
X404-1764-4001	Cn1c (C (=O) O) nnc1 [C@H] 1CCC [C@] (O) (c2ccc (O) cc2) C1
X404-1764-2345	Cc1cc (CNC2cccc2N2C [C@H] (c3ncn ([C@H] 4CC [C@H] (C (=O) O) CC4) s3) CC2=O) [nH] n1
X404-1764-0025	Oc1ccc (-c2cc (Nc3c (Cc4cccc4) on3) ccc2N2CCCO (O) (C (F) (F) CC2) ccl
X404-1764-2402	NCc1ccc (-c2nnc3sc (CN4CCN (S (=O) (=O) C5CC5) CC4) c23) ccl
X404-1764-3071	FC (F) (F) OC1 (CNc2ccnc (-c3cc4ccncc4 [nH] 3) n2) CCCCC1
X404-1764-4281	C [C@H] 1CN (Cc2nnc3ccc (NCC (C) (C) CC#N) cn23) CC2 (CCCC2) O1
X404-1760-0042	O=S1 (=O) Nc2c (-c3ccc (O [C@H] 4CNCC4 (F) F) nc3) cccc2N1Cc1cccc1C (F) (F) F
X404-1760-1189	O=C (O) c1cccc1-c1ccc (CN [C@H] 2CCC [C@H] 2NCC (F) (F) F) [nH] 1
X404-1760-0185	C [C@H] (NC (=O) CCC (F) (F) F) c1ccc (N2CC [C@H] (Nc3csc (-c4ccc (O) cc4) n3) C2) ccl
X404-1760-0023	O=C1CC2 (CCC2) CCN1C (=O) c1cc (-c2cc (C3CC (F) F) C3) c3cn [nH] c3n2) cc2ccccn12
X404-1761-3537	Cc1ccn2ncc (-c3cnc (N4CCC (N5CCC [C@H] 5C) CC4) o3) c2c1
X404-1760-0572	CNC [C@H] (O) c1ccc (C2 (CNC) CCCCC2) ccl
X404-1760-2143	COc1cc2n (n1) CCN (CC (=O) Nc1cccc3c1cc (N1CCOC [C@H] (C) C1) n3C) C2
X404-1768-5005	CC [C@H] (Nc1cn (C (C) C) c (=O) c1) c1ccc (-c2cccc (NC (=O) c3ccsn3) c2) ccl
X404-1760-1425	Cc1cc (N2CCC (c3cc (-c4ccc (F) cc4) on3) CC2) n (CCCS (C) (=O) =O) n1
X404-1761-2220	CCc1nc2c (-c3nccn3 [C@H] 3CN (C (=O) C4CC4) C [C@H] 3F) ccnc2 [nH] 1
X404-1761-4128	CCN (c1cccc ([C@H] (C) Nc2nc (=O) c (-c3cccc3) c [nH] 2) c1) S (C) (=O) =O
X404-1768-3704	Cc1cc (=O) nc (N (Cc2ccc (N3CC (C (F) F) C3) cc2) c2cccc (C#N) c2) [nH] 1

Table 6. URSA-expert-2026 set 2D structures.



As proof of the confirmed synthetic accessibility status of molecular structures in the URSA-expert-2026, we provide the example of a theoretical synthetic scheme proposed by synthetic organic chemistry experts (see Figure 20).

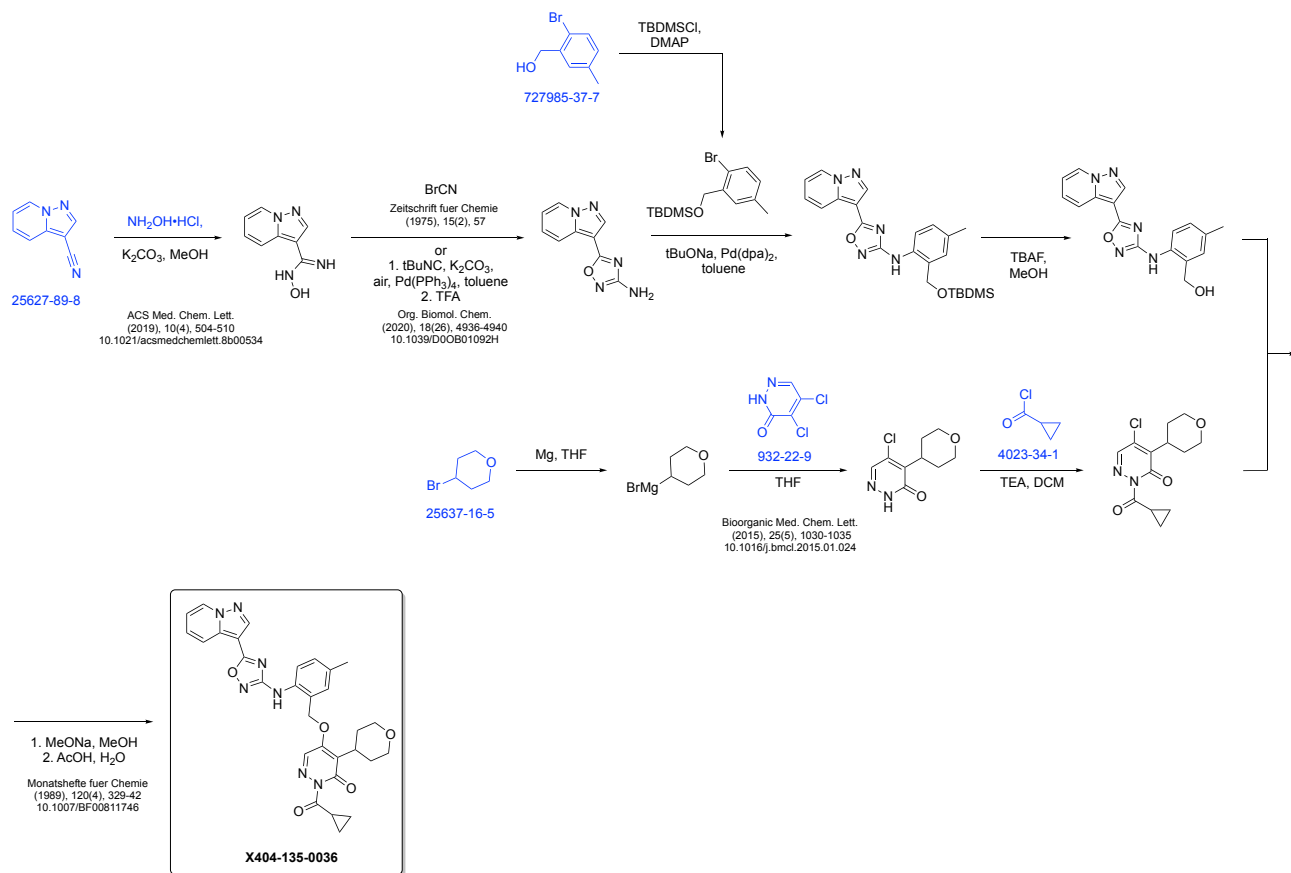


Figure 20. Theoretical synthesis scheme for the compound X404-135-0036 from URSA-expert-2026 set.

The URSA-expert-2026 was used as a holdout set. The CREED and USPTO-full were decontaminated within URSA-expert-2026, so the training datasets for our models don't contain reactions and product molecules from the holdout at all.

L. Benchmark Models Completions Examples

Most of the general purpose models we tested support reasoning, but the availability of reasoning traces differs. GPT(OpenAI, 2025a;b) models do not expose reasoning traces. Grok(xAI, 2025) exposes encrypted reasoning traces, so ordinary users cannot easily analyze them. DeepSeek 3.2 (DeepSeek-AI, 2025) does not support an explicit reasoning. Kimi-K2-thinking (Team, 2025c) has thinking traces, but does not expose them through API.

User input

Task: You are a helpful assistant in chemistry and biology. Your task is to predict the reactants that synthesize the given product. Carefully study previous conversation to match the exact output format. The SMILES strings in the final answer should be wrapped in <smiles>...</smiles> tags.

<Few-shot examples>.

Based on the given product, provide some plausible reactants that might have been utilized to prepare it.

Product: Cc1cccc(Nc2noc(-c3ccnn4cccccc34)n2)c(COc2ccnn(C(=O)C3CC3)c(=O)c2C2CCOCC2)c1
Return: Reasoning + Answer.

Model: Grok-4.1**Reasoning**

Not available

Answer

<smiles>Cc1ccc(Nc2noc(-c3cnn4cccc34)n2)c(COc2cnnC(=O)c2C2CCOCC2)c1. O=C(Cl)C1CC1 </smiles >

Model: Gemini 2.5 Flash**Reasoning**

Alright, let's break this down. My primary goal here is to identify potential synthetic routes to this complex molecule, focusing on plausible starting materials and key bond formations. The product is a beast! It's clear that I need to dissect this structure into manageable pieces.

First, I'm thinking about the central benzene ring. It acts like a hub, connecting several important fragments. This ring contains an amine group (N-aryl linkage) and an ether linkage (-CH₂O-). That amine is likely formed via Buchwald-Hartwig amination or Ullmann condensation. The ether, an SN₂ reaction or a Williamson ether synthesis or something similar, and I'll need to figure out which reaction is most suitable.

Now, let's look at the fragments. The left side of the nitrogen - the 'Nc2noc(-c3cnn4cccc34)n2' fragment – looks like an oxadiazole ring fused to a benzotriazole-like system – an imidazobenzotriazole derivative. That amino-oxadiazole ring, 'Nc2noc(-c3cnn4cccc34)n2' may be formed from an amidoxime and an acyl chloride derivative. The oxadiazole itself can be built from amidoximes and then coupled to the complex heterocycle.

The right side, 'COc2cnn(C(=O)C3CC3)c(=O)c2C2CCOCC2', is a pyrazolone with a cyclopropane carbonyl and a tetrahydropyran. This is a pyrazolone derivative. This structure contains a carbonyl and likely made via standard pyrazolone synthesis using a beta-keto ester and a hydrazine derivative.

To summarize, for the N-aryl bond, I could see using a Buchwald-Hartwig amination approach. For example, a bromo-benzene derivative and the oxadiazole-containing amine. For the ether linkage, I anticipate the reaction between an alcohol and an aryl halide, or the alcohol version of the central aryl fragment and the pyrazolone derivative that is being attached.

Answer

The complex structure of the given product suggests a multi-step synthesis involving several key transformations. We can deduce plausible reactants by breaking down the product into simpler, recognizable fragments and considering common synthetic reactions for their formation and subsequent coupling. Product: <smiles> Cc1ccc(Nc2noc(-c3cnn4cccc34)n2)c(COc2cnn(C(=O)C3CC3)c(=O)c2C2CCOCC2)c1 </smiles>

Let's break down the molecule:

1. **Central Phenyl Core:** 'Cc1ccc(N...c(CO...))c1'
2. **Left Arm (N-aryl-oxadiazole-heterocycle):** 'Nc2noc(-c3cnn4cccc34)n2'
3. **Right Arm (Ether-linked pyrazolone derivative):** 'COc2cnn(C(=O)C3CC3)c(=O)c2C2CCOCC2'

Based on this, we can propose the following disconnections:

Disconnection 1: N-aryl bond formation The N-aryl bond ('Ar-NH-Ar') is commonly formed via a Buchwald-Hartwig amination or Ullmann condensation. This would involve an aryl halide and an amine.

<skipped reasoning>

Let's define the two major fragments:

Fragment A (Amine component): 'H2N-c1noc(-c2cnn3cccc23)n1' This is a 5-amino-1,2,4-oxadiazole derivative. The '-c2cnn3cccc23' group is likely a '[1,2,4]triazolo[4,3-a]quinoline' or similar bicyclic nitrogen heterocycle. Let's call this 'R_A'. A common synthesis for 5-amino-1,2,4-oxadiazoles involves reacting an amidoxime ('R-C(=NOH)NH2') with cyanogen halide ('Cl-CN') or similar reagent, or reacting a nitrile ('R-CN') with hydroxylamine to form the amidoxime, followed by cyclization. So, 'R_A-CN' (e.g., '[1,2,4]triazolo[4,3-a]quinoline-CN') and 'NH2OH' (hydroxylamine) could be precursors to the 'R_A-C(=NOH)NH2' which then forms 'H2N-c1noc-R_A'.

Fragment B (Phenolic component): 'HO-c1cnn(C(=O)C2CC2)c(=O)c1C1CCOCC1' This is a '1H-pyrazole-5-ol' or '5-hydroxypyrazole' derivative. The keto-enol tautomerism of pyrazolones is relevant here. The core pyrazolone ring ('N-N=C-C(=O)-C') is often formed by the condensation of a beta-keto ester with a hydrazine derivative. In this case, the pyrazolone has:

- * An N-substituent: 'C(=O)C2CC2' (cyclopropylcarbonyl)
- * A C-substituent: 'C1CCOCC1' (tetrahydropyran-4-yl)

 So, a possible formation route for Fragment B could involve:

1. **Hydrazine derivative:** 'H2N-NH-C(=O)C2CC2' (N-cyclopropylcarbonyl hydrazine)
2. **Beta-keto ester:** 'R-CO-CH2-COOEt' where 'R' is 'C1CCOCC1' (ethyl 3-oxo-3-(tetrahydropyran-4-yl)propanoate)

<skipped reasoning>

Overall Proposed Reactants:

The most direct disconnection leads to three main fragments that are then coupled.

* **Fragment 1 (central core with leaving group for N-arylation and a nucleophilic alcohol for etherification):** <smiles>Cc1ccc(Br)c(CO)c1</smiles>

* **Fragment 2 (amino-oxadiazole):** <smiles>Nc1noc(-c2cnn3cccc23)n1</smiles> (This compound itself might be synthesized from '[1,2,4]triazolo[4,3-a]quinoline-3-carbonitrile' and hydroxylamine, followed by cyanation and cyclization).

* **Fragment 3 (hydroxypyrazolone):** <smiles>Oc1cnn(C(=O)C2CC2)c(=O)c1C1CCOCC1</smiles> (This compound can be synthesized from 'H2N-NH-C(=O)C2CC2' and 'ethyl 3-oxo-3-(tetrahydropyran-4-yl)propanoate').

Given the complexity, a multi-step synthesis would be required. One possible sequence:

1. Buchwald-Hartwig coupling of 'Cc1ccc(Br)c(CO)c1' with 'Nc1noc(-c2cnn3cccc23)n1' to form the N-aryl bond. This would yield <smiles>Cc1ccc(Nc2noc(-c3cnn4cccc34)n2)c(CO)c1</smiles>.
2. Then, a Mitsunobu reaction or a Williamson ether synthesis between the benzylic alcohol ('-CH2OH') from the product of step 1 and the phenolic pyrazolone ('Oc1cnn(C(=O)C2CC2)c(=O)c1C1CCOCC1'). For Williamson, the alcohol would first be converted to a bromide, then reacted with the phenol.

Therefore, the likely direct reactants for the final coupling steps are:

<smiles>Cc1ccc(Nc2noc(-c3cnn4cccc34)n2)c(CO)c1</smiles>

<smiles>Oc1cnn(C(=O)C2CC2)c(=O)c1C1CCOCC1</smiles>

Model: Gemini 3 Flash preview

Reasoning

Parsing the Structure

Now, I'm carefully dissecting the pyrazolone-containing fragment, attempting to identify each atom's bonding. It seems that the key to understanding the structure lies in correctly interpreting the ring closure within the SMILES string. I'm focusing on the position of the tetrahydropyran substituent.

Answer

<smiles >Cc1ccc(Nc2noc(-c3cnn4cccc34)n2)c(CO)c1. O=C(c1cnn(C(=O)C2CC2)c(=O)c1C1CCOCC1)O </smiles >

Model: GPT 5.1

Reasoning

Not available

Answer

<smiles >Cc1ccc(N)c(COc2cnn(C(=O)C3CC3)c(=O)c2C2CCOCC2)c1.c1noc(-c2cnn3cccc23)n1Cl</smiles >

Model: GPT 5.2

Reasoning

Not available

Answer

<smiles >Cc1ccc(N)c(COc2cnn(C(=O)C3CC3)c(=O)c2C2CCOCC2)c1.Clc1noc(-c2cnn3cccc23)n1</smiles >

Model: Claude 4.5 Sonnet**Reasoning**

Let me analyze this complex molecule step by step to identify potential reactants.

The product is: <smiles>Cc1ccc(Nc2noc(-c3cnn4cccc34)n2)c(COc2cnn(C(=O)C3CC3)c(=O)c2C2CCOCC2)c1</smiles>

Let me break down the structure: 1. There's a methylated benzene ring with an NH group connected to an oxadiazole 2. The oxadiazole has a 1H-indazole substituent 3. The benzene also has a CH2O- linker connecting to a pyridazinone 4. The pyridazinone has a cyclopropylcarbonyl group on the nitrogen 5. The pyridazinone also has a tetrahydropyran substituent

Looking at the structure, this appears to be formed from multiple coupling reactions. Let me identify potential disconnection points:

1. The NH-oxadiazole bond could be formed via nucleophilic aromatic substitution 2. The CH2O ether linkage could be formed via Williamson ether synthesis 3. The cyclopropylcarbonyl on the nitrogen could be an acylation

Key fragments I can identify: - The oxadiazole with indazole: -c1noc(-c2cnn3cccc23)n1 - The aromatic amine with CH2OH: Cc1ccc(N)c(CO)c1 or similar - The pyridazinone core with substituents

Let me think about the most likely disconnections:

The most straightforward synthesis would involve: 1. A substituted benzene with NH2 and CH2O- groups 2. An oxadiazole electrophile (likely with a leaving group like Cl) 3. A pyridazinone with an OH group that can react with the CH2 group

The most probable route involves coupling an aniline bearing the CH2O-pyridazinone moiety with a chloro-oxadiazole intermediate. Alternatively, the oxadiazole-aniline coupling could occur first, followed by attachment of the pyridazinone through the CH2 linker, about which is more likely. The first option seems more straightforward: the aniline nitrogen would perform a nucleophilic aromatic substitution on the chloro-oxadiazole, displacing the chlorine and forming the N-aryl bond directly.

Answer

Looking at this complex molecule, I can identify key disconnection points. The most likely synthesis involves:

1. A nucleophilic aromatic substitution between an aniline and a chloro-oxadiazole 2. The aniline already contains the CH2O-pyridazinone substituent

Plausible reactants:

<smiles>Cc1noc(-c2cnn3cccc23)n1</smiles>

<smiles>Cc1ccc(N)c(COc2cnn(C(=O)C3CC3)c(=O)c2C2CCOCC2)c1</smiles>

The reaction would proceed via nucleophilic aromatic substitution where the aniline nitrogen attacks the chloro-oxadiazole, displacing the chloride leaving group.

Model: Claude 4.5 Opus

Reasoning

Let me analyze the product structure to determine possible reactants.

Product SMILES: Cc1ccc(Nc2noc(-c3cnn4cccc34)n2)c(COc2cnn(C(=O)C3CC3)c(=O)c2C2CCOCC2)c1

This is a complex molecule. Let me break it down:

1. There's a methylphenyl group (toluene derivative) with: - A -Nc2noc(-c3cnn4cccc34)n2 substituent (an oxadiazole ring with an indazole) - A -COc2cnn(C(=O)C3CC3)c(=O)c2C2CCOCC2 substituent (a pyridazinone with cyclopropyl amide and tetrahydropyran)

Looking at this structure, I can see several key components:

1. An oxadiazole ring (-noc-n-) connected to: - An aniline nitrogen - An indazole (-c3cnn4cccc34)
2. A pyridazinone system with: - An ether linkage (COc) - A cyclopropyl carbonyl group C(=O)C3CC3 - A tetrahydropyran ring (C2CCOCC2)

Possible disconnections: 1. The ether bond (C-O-C) between the benzyl and pyridazinone 2. The C-N bond between the aniline and oxadiazole

For the synthesis, plausible reactants could be:

1. A halogenated pyridazinone (like a chloropyridazinone): Clc1cnn(C(=O)C2CC2)c(=O)c1C1CCOCC1
2. A hydroxymethyl-substituted aniline bearing the oxadiazole group: HOCc1cc(C)ccc1Nc2noc(-c3cnn4cccc34)n2

The key disconnections appear to be the ether linkage between the benzyl carbon and pyridazinone oxygen, and potentially the C-N bond connecting the aniline to the oxadiazole. A nucleophilic aromatic substitution or Williamson ether synthesis could couple these fragments together. =O at the ring, and a tetrahydropyran substituent attached. For an ether formation reaction, I need an alcohol group and a halide leaving group. The benzyl alcohol from the aniline-oxadiazole compound would serve as the nucleophile, while the chlorine on the pyridazinone ring would act as the leaving group in a Williamson ether synthesis.

Let me map out the reactants more carefully. The first component contains the methylated aromatic ring with the aniline linker and indazole moiety, terminating in a primary alcohol. The second reactant is the chlorinated pyridazinone with the cyclopropyl carbamate and tetrahydropyran groups. Now I need to properly encode these structures—let me verify the connectivity by working through the product structure systematically, starting from the central benzene ring and tracing each substituent to ensure the SMILES representation is accurate.

=O)c1C1CCOCC1

Converting to SELFIES format requires careful parsing of the SMILES notation. The chloropyridazinone reactant has a pyridazinone core with a cyclopropyl carbamate substituent and a morpholine ring attached. I'll work through the SMILES systematically to ensure accurate conversion, starting with the alcohol component and then the chlorinated pyridazinone to map out the ether bond formation properly. The indazole is fused to a benzene ring, and there's a hydroxymethyl substituent on the benzene. For the chloropyridazinone component, I have chlorine on the ring itself, an N-cyclopropylcarbonyl group, and a tetrahydropyran moiety attached. Converting these structures to SELFIES notation for the final answer.)n2)c(CO)c1 for the benzyl alcohol derivative. For the chloropyridazinone, I need to verify the structure matches the product fragment where the oxygen connects to the pyridazinone ring. The reactant should have a chloride at that position: Clc1cnn(C(=O)C3CC3)c(=O)c1C1CCOCC1. I'm reconsidering the ring numbering to ensure the connectivity is correct for the coupling reaction. The chlorinated pyridazinone can be written more concisely as Clc1cnn(C(=O)C2CC2)c(=O)c1C1CCOCC1, which clearly shows the chlorine substituent, the cyclopropyl carbonyl group on one nitrogen, the carbonyl making it a pyridazinone, and the tetrahydropyran ring attached to the aromatic core.

Answer

Looking at the product structure, I can identify a key ether linkage (C-O-C) between the benzyl group and the pyridazinone ring. This suggests a nucleophilic substitution reaction between a benzyl alcohol and a halogenated pyridazinone.

The product can be disconnected into: 1. A benzyl alcohol containing the oxadiazole-indazole moiety 2. A chloropyridazinone with the cyclopropyl amide and tetrahydropyran substituents

<smiles>Cc1ccc(Nc2noc(-c3cnn4cccc34)n2)c(CO)c1 </smiles>
<smiles>Clc1cnn(C(=O)C2CC2)c(=O)c1C1CCOCC1 </smiles>

Model: DeepSeek 3.2

Reasoning

Not available

Answer

Based on the structure analysis, the product likely results from a Buchwald-Hartwig amination coupling between an aniline derivative and a halogenated heterocycle. The plausible reactants are:

<smiles>Cc1ccc(NH2)c(COc2cnn(C(=O)C3CC3)c(=O)c2C2CCOCC2)c1 </smiles><smiles>Clc2noc(-c3cnn4cccc34)n2 </smiles>

Model: Kimi K2

Reasoning

Not available

Answer

<smiles>Cc1ccc(Nc2noc(-c3cnn4cccc34)n2)c(CBr)c1 </smiles>
<smiles>Oc1cnn(C(=O)C2CC2)c(=O)c1C1CCOCC1 </smiles>

Model: RetroDFM-R**Reasoning**

The target molecule, 2-(cyclopropanecarbonyl)-5-[[5-methyl-2-[(5-pyrazolopyridinyl-1,2,4-oxadiazol-3-yl)amino]phenyl]methoxy]-4-(tetrahydropyran-4-yl)pyridazin-3-one, features several critical functional groups: (1) a pyridazinone ring with a tetrahydropyran substituent, (2) a substituted benzene ring bearing an oxadiazole-linked anilino group, and (3) a cyclopropanecarbonylamino group on the pyridazinone nitrogen. Retrosynthetically, the acyl group (cyclopropanecarbonyl) on the pyridazinone nitrogen is disconnected via amide bond formation. This suggests the precursor pyridazinone compound with a free NH group reacts with cyclopropanecarbonyl chloride under basic conditions to form this acylation step. The ether linkage (methoxy group) on the benzene-pyridazinone backbone may arise earlier from a Williamson ether synthesis. However, the ground-truth reactants indicate the ether structure is preassembled in one precursor. Thus, the synthesis likely prioritizes installing the ether via alkylation/arylation before introducing the acyl group on the nitrogen. However, the ground-truth reactants already incorporate this ether, implying this strategy was pre-installed during their assembly.

The proposed disconnection focuses on the acylation step. Amide formation via acylation with cyclopropanecarbonyl chloride under Schotten-Baumann-type conditions (e.g., pyridine) ensures efficient coupling with nucleophilic attack. This pathway aligns well with the ground-truth reactants provided. Steric and electronic factors (e.g., pyridazinone's resonance structure influencing NH reactivity) are mitigated using coupling reagents or elevated temperatures to drive selectivity. This retrosynthetic approach avoids side reactions (e.g., over-chloroformylation) due to steric hindrance around the pyridazinone ring. This two-component approach (pre-assembled ether intermediate and cyclopropanecarbonyl electrophile) provides a robust, modular strategy with compatibility to aromatic ether formation, while maintaining regiochemical control. The approach aligns with the provided ground-truth reactants, validating this disconnection's feasibility.

Answer
Cc1ccc(Nc2noc(-c3cnn4cccc34)n2)c(COc2cn[nH]c(=O)c2C2CCOCC2)c1.C(=O)(Cl)C1CC1
Model: NatureLM**Reasoning**

Not available

Answer
<reactants>Cc1ccc(Nc2noc(-c3cnn4cccc34)n2)c(COc2cn[nH]c(=O)c2C2CCOCC2)c1.C(=O)(Cl)C1CC1</reactants>

Model: ether0**Reasoning**

Okay, let's see... The user is asking about a chemical molecule and wants a one-step synthesis from purchasable precursors. The SMILES for the target molecule is: Cc1ccc(N-c2noc(-c3cnn4cccc34)n2)c(CO-c2cnn(C(=O)C3CC3)c(=O)c2C2CCOCC2)c1.

The SMILES notation is complex, indicating multiple rings connected together. The target molecule is likely a substituted benzimidazole or similar heterocycle with functional groups, including an ether, ketone, and cyclopropane rings.

The user is suggesting a reaction involving multiple components. The challenge is to find a reaction that can produce the specified compound from purchasable materials in one step.

Common reactions include nucleophilic substitutions, amide couplings, or condensation reactions. The presence of nitrogen-containing rings suggests a amine-based coupling reaction. The molecule already has N attached directly to benzene rings, suggesting a aniline or diaryl amine.

The structure could be a coupling between an aryl halide and a complex amine via a coupling reaction. The target has a complex structure with multiple rings and substituents, including an N-substituted aryl ether or amide linkage.

The main benzene ring (c1cccc1) has a methyl substituent, a nitro group, and a substituent with amine linked to another ring. The benzene ring is Cc1ccc(...c(CO...)), implying position 4 with a methyl group and an activating groups like CCO or O connected through an ether linkage at the 4-position.

Considering reactions:

1. **SNAr** (substituent on aromatic rings): - Benzene substituents can undergo coupling reactions, like substitution of an existing leave group with an amine subsequent from another carbonyl or bromide source. - Multiple electron-withdrawing groups activate the ring and allow substitution.

2. **Benzimidazole** derivatives can be formed via a C-N bond formation: - The amine and aryl chloride or halide could attach to form a substituting amine. - Perhaps a Buchwald–Hartwig amination?

Possible precursors: The first part is the source molecule, and the second component is the amine. Given the complexity, the reaction likely links these parts.

Reaction Component: The most plausible reaction is forming an ether linkage (COgene) or a condensation between a ketone and amine groups:

The original reaction components might be: CO or COc2cnn(C(=O)C3CC3)c(=O)c2C2CCOCC2 succinctly suggesting a one possibility of linking substituents via coupling.

The succinct reaction SMILES: Cc1ccc(Br)c(CO-c2cnn(C(=O)C3CC3)c(=O)c2C2CCOCC2)c1.N-c2noc(-c3cnn4cccc34)n2;[Cu];Cc1ccc(N-c2noc(...n2)c(CO-c2...)).

Answer

Cc1ccc(Br)c(COc2cnn(C(=O)C3CC3)c(=O)c2C2CCOCC2)c1.N-c2noc(-c3cnn4cccc34)n2;[Cu];Cc1ccc(N-c2noc(-c3cnn4cccc34)n2)c(CO-c2cnn(C(=O)C3CC3)c(=O)c2C2CCOCC2)c1

Model: C3LM, SFT, C3LM+USPTO-full, no reasoning**Reasoning**

Not available

Answer

<smiles>O=C(C1CC1)n1c(=O)c(C2CCOCC2)c(OCc2c(N)ccc(C)c2)cn1.c12c(-c3nc(Cl)no3)cnn1cccc2</smiles>

Model: C3LM, RFT, CC reward

Reasoning

Not available

Answer

<smiles>c1ccc2c(-c3onc(Nc4ccc(C)cc4COc4c(C5CCOCC5)c(=O)n(C(=O)C5CC5)nc4)n3)c(Cl)nn2c1</smiles>